Materials Design
2024 UGM Webinar Series

VASP: Present and Future

VASP GmbH

University of Vienna

November 5, 2024

Materials Design UGM

UGM 2024

The Materials Design annual user event will be online for 2024.

Tuesdays and Thursdays
October 15 – November 7

Plenary Speakers:

Professor Sir Richard Catlow - University College London, England
Professor Georg Kresse, Dr. Martijn Marsman,
and Dr. Manuel Engel - The University of Vienna, Austria
Professor Greg Olson - Massachusetts Institute of Technology, USA
Dr. Céline Chizallet - IFP Energies Nouvelles, France

https://ugm.materialsdesign.com/

materials design

Materials Design
2024 UGM Webinar Series

VASP: Present and Future

VASP GmbH

University of Vienna

universität wien

VASP

November 5, 2024

Webinar Speakers

Katherine Hollingsworth

Dr. Volker Eyert

Materials Design UGM Presenters

Dr. Manuel Engel
VASP GmbH

Dr. Martijn Marsman
VASP GmbH
University of Vienna

Materials Design UGM Webinar Series

- Share the plenary sessions with your colleagues!
  - Registration details

    https://www.ugm.materialsdesign.com
- We will be recording this session
  - Upcoming sessions are posted on the UGM site
  - Watch any of our earlier webinars anytime www.materialsdesign.com/webinars
- Brief survey
  - Take a 2 minutes brief survey at the end of the webinar
- Audio issues
  - Log out and log back in again
  - Check your audio output
  - Google Chrome (most recent 2 versions) Mozilla Firefox (most recent 2 versions) Apple Safari (most recent 2 versions) Microsoft Edge (most recent 2 versions)

materials design

Please Ask Questions!

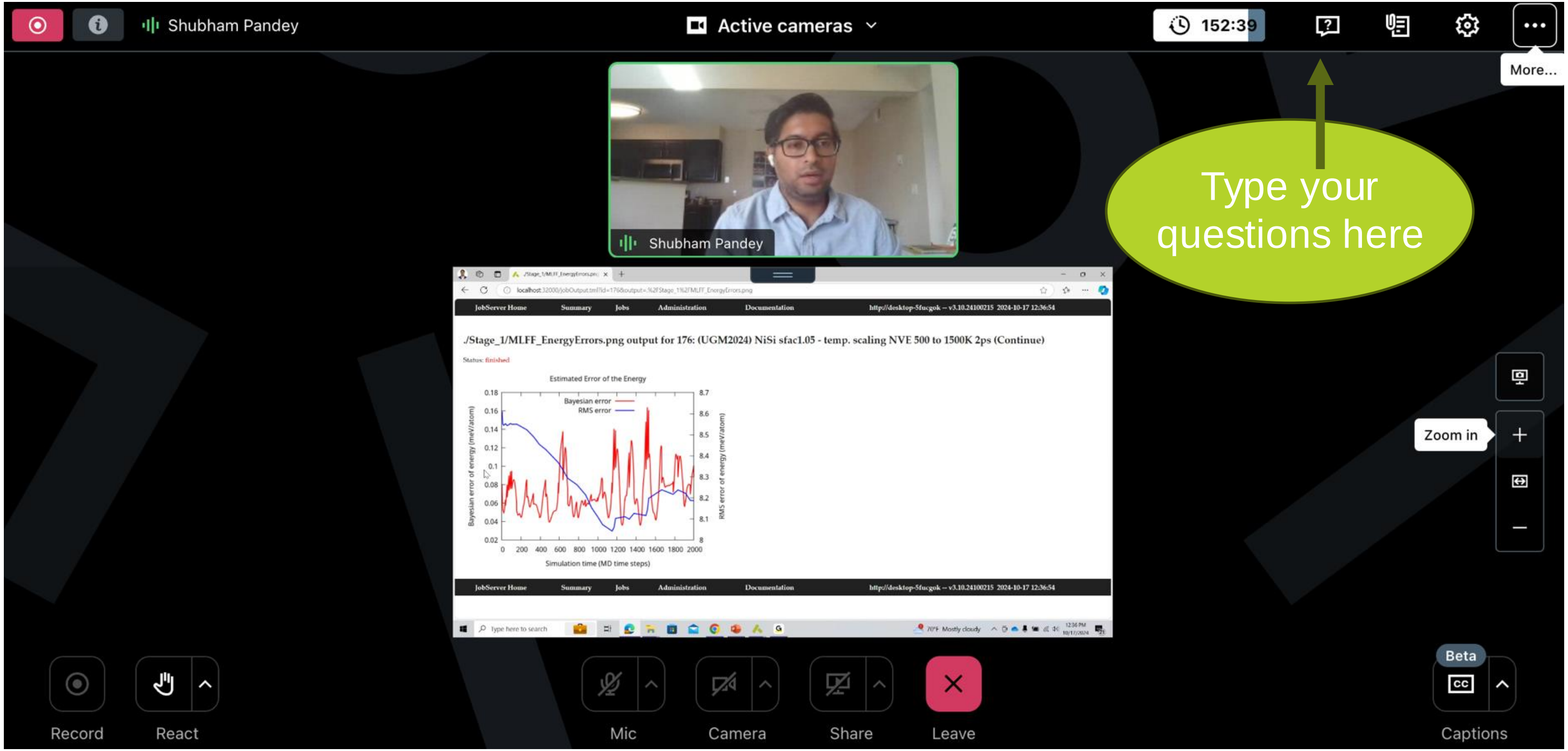

materials design

New in VASP

Electron-Phonon Interactions

Manuel Engel

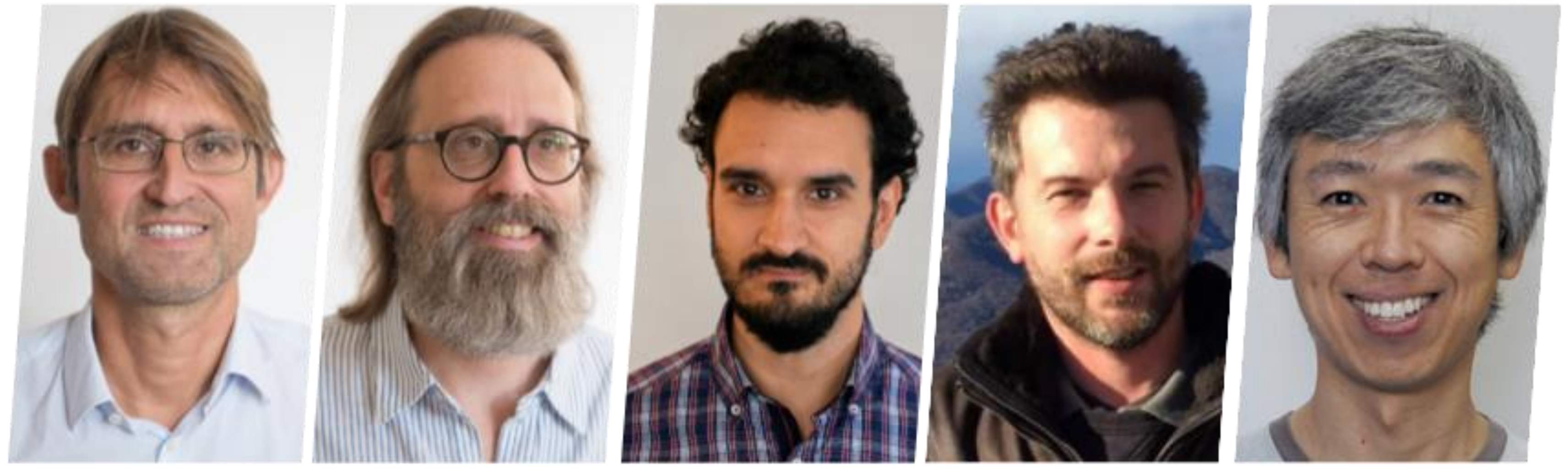

Materials Design
User Group Meeting 2024

Outline

Electron-Phonon Coupling

Method and Workflow

Electron Self-Energy

Band-Structure Renormalization

Transport Properties

Features

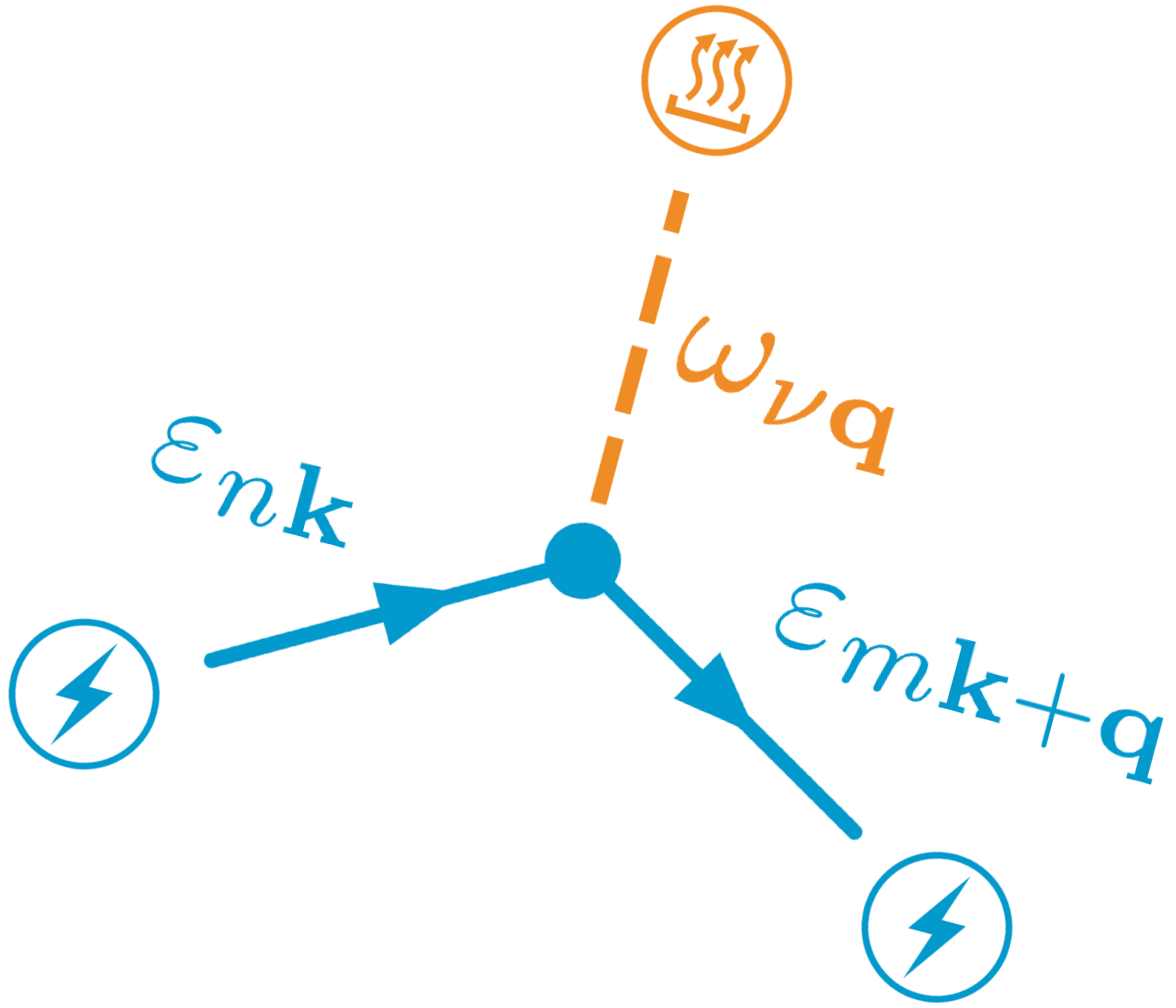

Phonons

Vibrations in atomic crystal structure

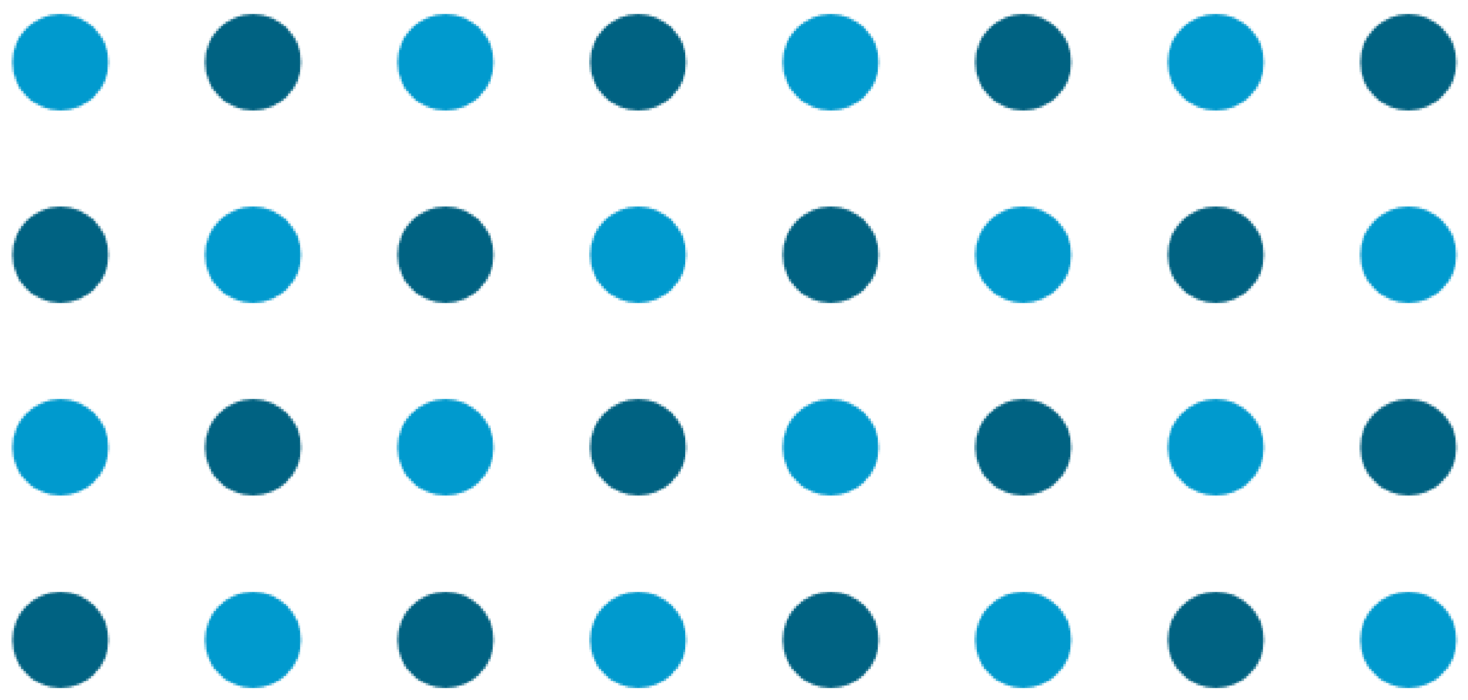

Rigid equilibrium configuration

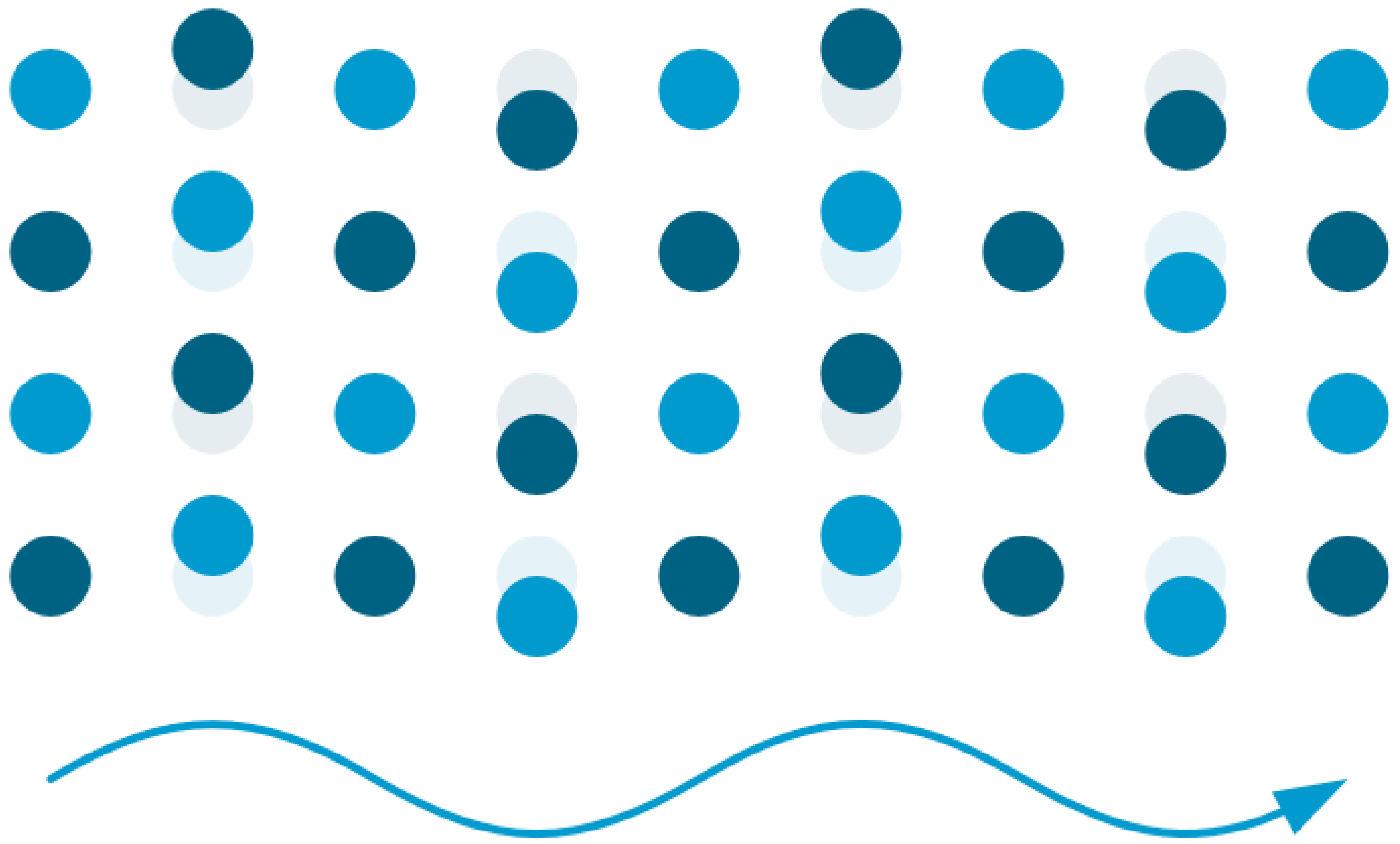

Traveling "phonon" wave
carries heat and sound

Electron-Phonon Interactions

Electron-Phonon Matrix Elements

The fundamental building blocks of electron-phonon interactions

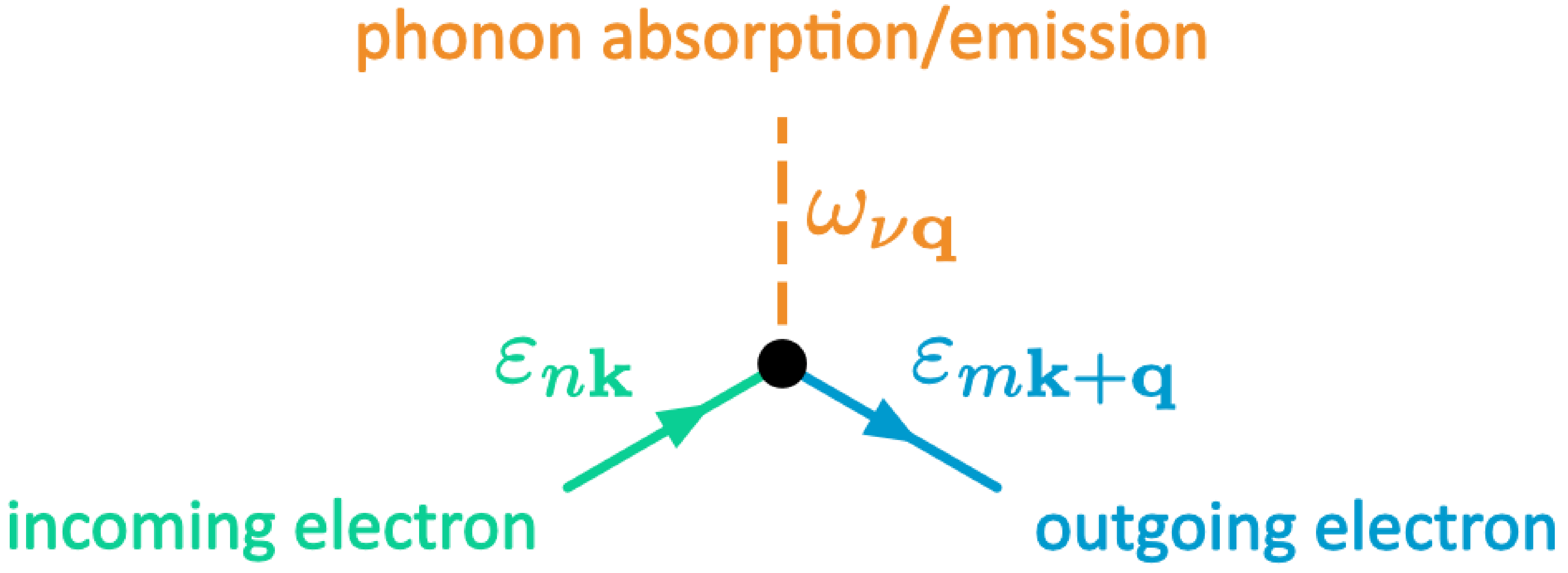

$$g_{mn\mathbf{k},\nu\mathbf{q}} \equiv \langle \Psi_{m\mathbf{k}+\mathbf{q}} | \partial_{\nu\mathbf{q}} \hat{H} | \Psi_{n\mathbf{k}} \rangle$$

F. Giustino, Rev. Mod. Phys. 89, 015003 (2017)

Supercell Method

Supercell

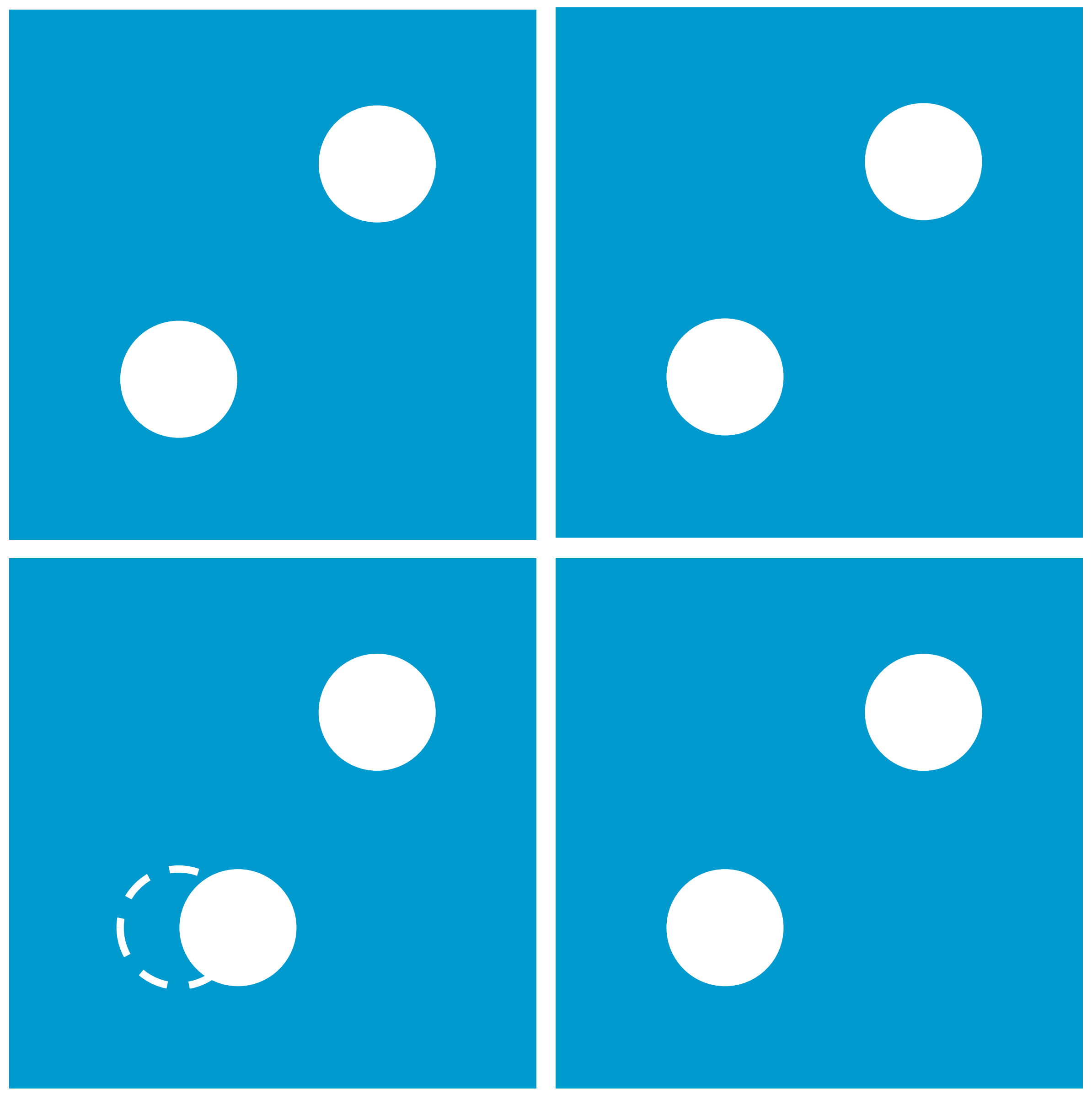

Finite atomic displacements

We can use **almost any density functional!**

$$\langle \mathbf{r}|\frac{\partial \hat{H}}{\partial \mathbf{u}_{p\kappa}}|\mathbf{r}\rangle = \frac{\partial V_{\mathrm{KS}}(\mathbf{r})}{\partial \mathbf{u}_{p\kappa}}$$

Interpolation procedure

Fast, accurate and robust

No Wannier functions required!

Unit cell

Bloch orbitals obtained **non-self-consistently** in the unit cell

L. Chaput, A. Togo, and I. Tanaka, Phys. Rev. B 100, 174304 (2019)

M. Engel, H. Miranda, L. Chaput, *et al.*, Phys. Rev. B 106, 094316 (2022)

Powerful Workflows

Pure VASP workflow

- Uses `IBRION=6` for finite displacements
- No external dependencies
- Simple to setup and run

VASP + python (velph/phelel)

- *velph* sets up calculations
- One VASP calculation per displacement
- *phelel* calculates derivatives
- Maximum flexibility

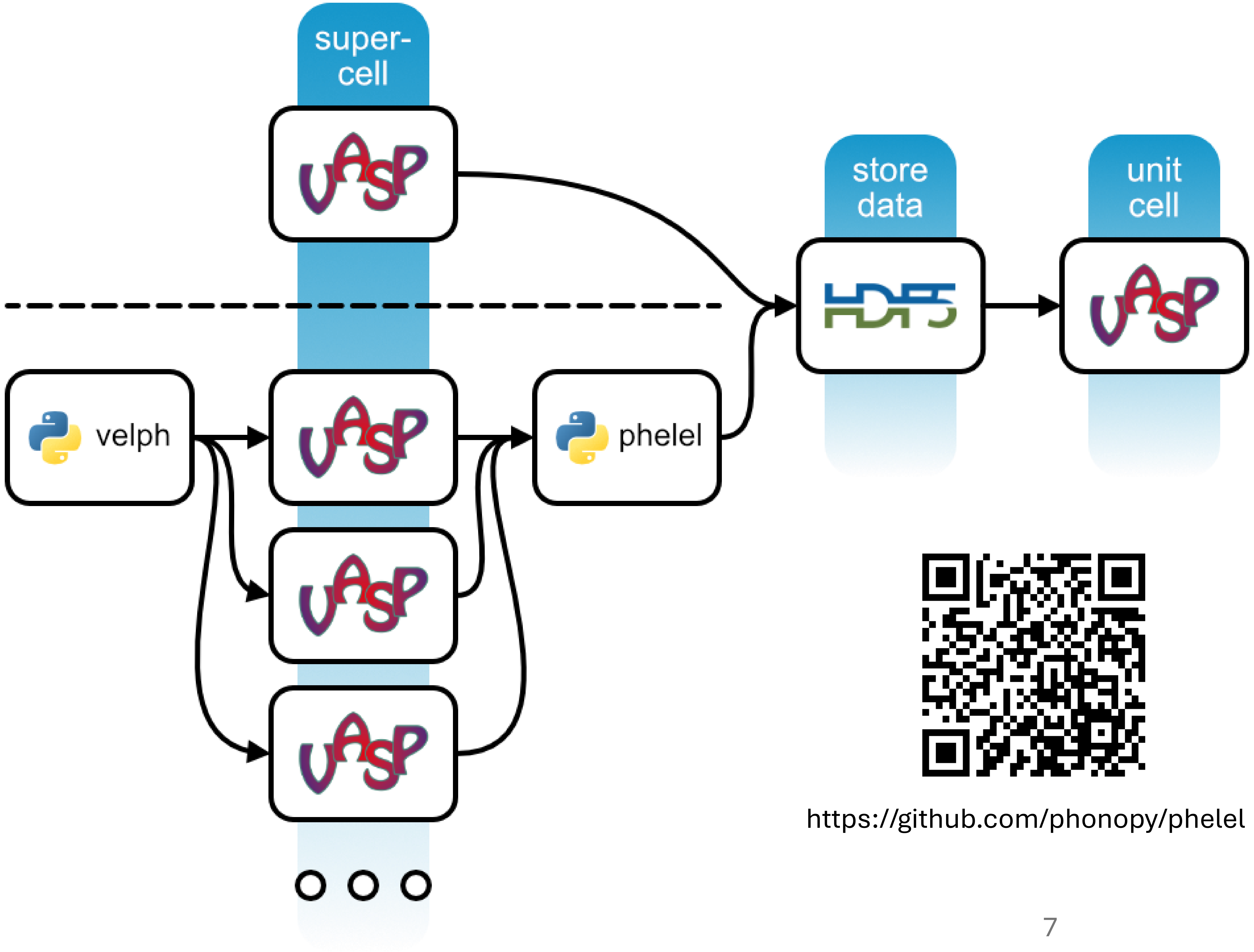

https://github.com/phonopy/phelel

Electron Self-Energy

Use perturbation theory to calculate self-energy (SE).
Real part of SE gives renormalization of band structure.

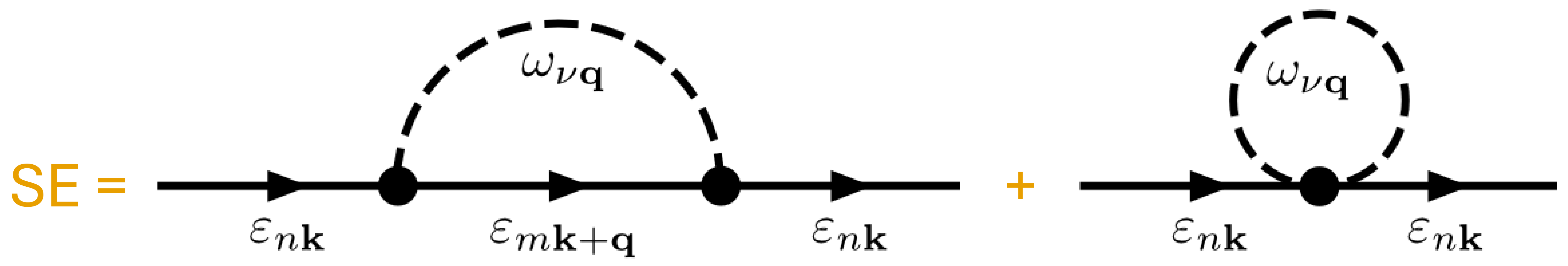

Fan-Migdal Debye-Waller

Effect even at zero Kelvin:
Zero-point renormalization (ZPR)

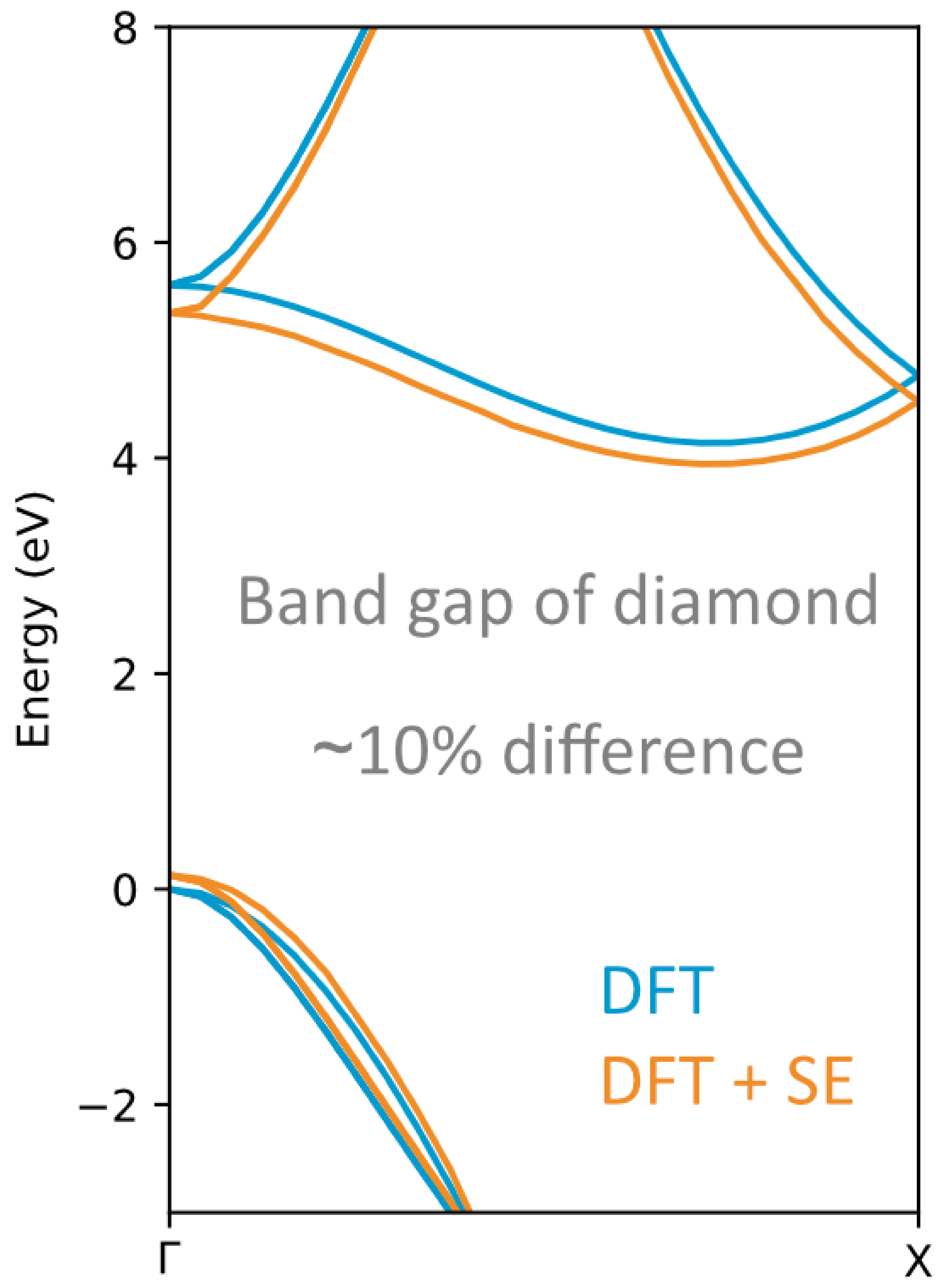

P. B. Allen and V. Heine, J. Phys. C: Solid State Phys. 9, 2305 (1976)
P. B. Allen and M. Cardona, Phys. Rev. B 23, 1495 (1981)

ZPR of the Band Gap

Material	ZPR* this work	ZPR* Ref.**	Rel. diff.
AlAs-zb	-74	-74	0.0 %
AlN-w	-377	-399	5.5 %
AlP-zb	-96	-93	3.2 %
BN-zb	-402	-406	1.0 %
BaO-rs	-277	-271	2.2 %
C-dia	-323	-330	2.1 %
CaO-rs	-357	-341	4.7 %
CdS-zb	-67	-70	4.3 %
CdSe-zb	-29	-34	14.7 %
CdTe-zb	-19	-20	5.0 %
GaN-w	-171	-189	9.5 %
GaN-zb	-163	-176	7.4 %
GaP-zb	-61	-65	6.2 %

Material	ZPR* this work	ZPR* Ref.**	Rel. diff.
Li2O	-569	-573	0.7 %
LiF-rs	-1231		
MgO-rs	-533	-524	1.7 %
Si-dia	-57	-56	1.8 %
SiC-zb	-175	-179	2.2 %
SiO2-t	-583	-585	0.3 %
SnO2-t	-232	-215	7.9 %
SrO-rs	-323	-326	0.9 %
TiO2-t	-349	-337	3.6 %
ZnO-w	-175	-157	10.2 %
ZnS-zb	-88	-88	0.0 %
ZnSe-zb	-43	-44	2.3 %

huge ZPR
> 1eV

* ZPR in meV

M. Engel, H. Miranda, L. Chaput, *et al.*, Phys. Rev. B 106, 094316 (2022)

Long-Range Electrostatic Effects

Electron-phonon matrix elements corresponding to LO phonon modes diverge in polar materials.

Requires proper treatment of long-range (LR) components of matrix elements (dipole interaction).

$$g^{\mathrm{LR}}_{mn\mathbf{k},\nu\mathbf{q}} \equiv \mathrm{i}\frac{4\pi}{V_{\mathrm{pc}}}\sum_{\kappa}\sqrt{\frac{\hbar}{2m_\kappa\omega_{\nu\mathbf{q}}}}\sum_{\substack{\mathbf{G}\neq-\mathbf{q}\\ \mathbf{K}\equiv\mathbf{q}+\mathbf{G}}}^{\mathrm{pc}}\frac{\mathbf{K}^{\top}\mathbf{Z}^{\star}_{\kappa}\mathbf{e}_{\kappa,\nu\mathbf{q}}}{\mathbf{K}^{\top}\boldsymbol{\epsilon}^{\infty}\mathbf{K}} \times \langle\psi_{m\mathbf{k}+\mathbf{q}}|\mathrm{e}^{\mathrm{i}\mathbf{K}\cdot(\hat{\mathbf{r}}-\tau_\kappa)}|\psi_{n\mathbf{k}}\rangle$$

$\mathbf{Z}^{\star}_{\kappa}$ ... Born effective-charge tensor
$\boldsymbol{\epsilon}^{\infty}$ ... Ion-clamped static dielectric tensor

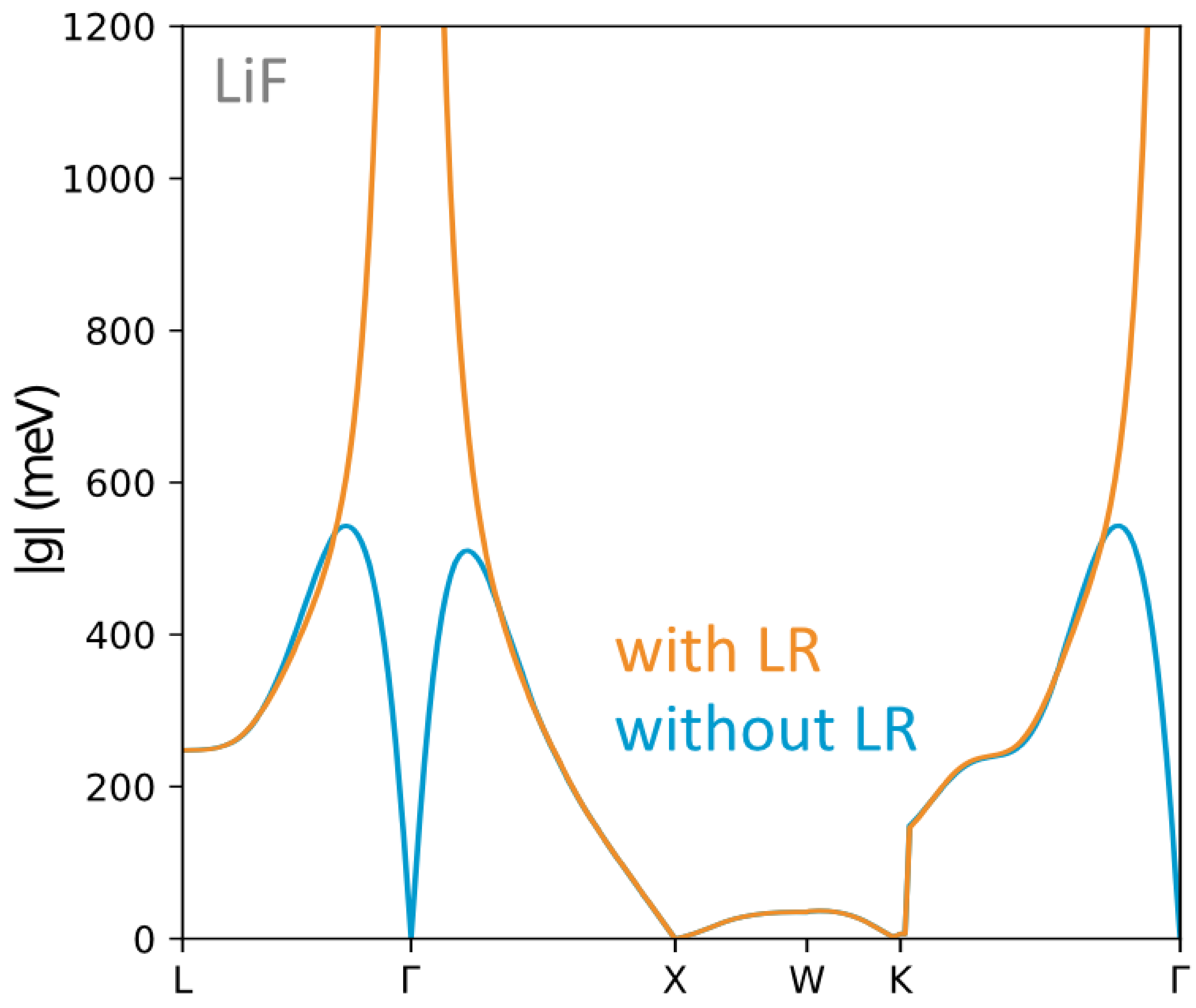

C. Verdi and F. Giustino, Phys. Rev. Lett. 155, 176401 (2015)

Temperature-dependent Band Gap

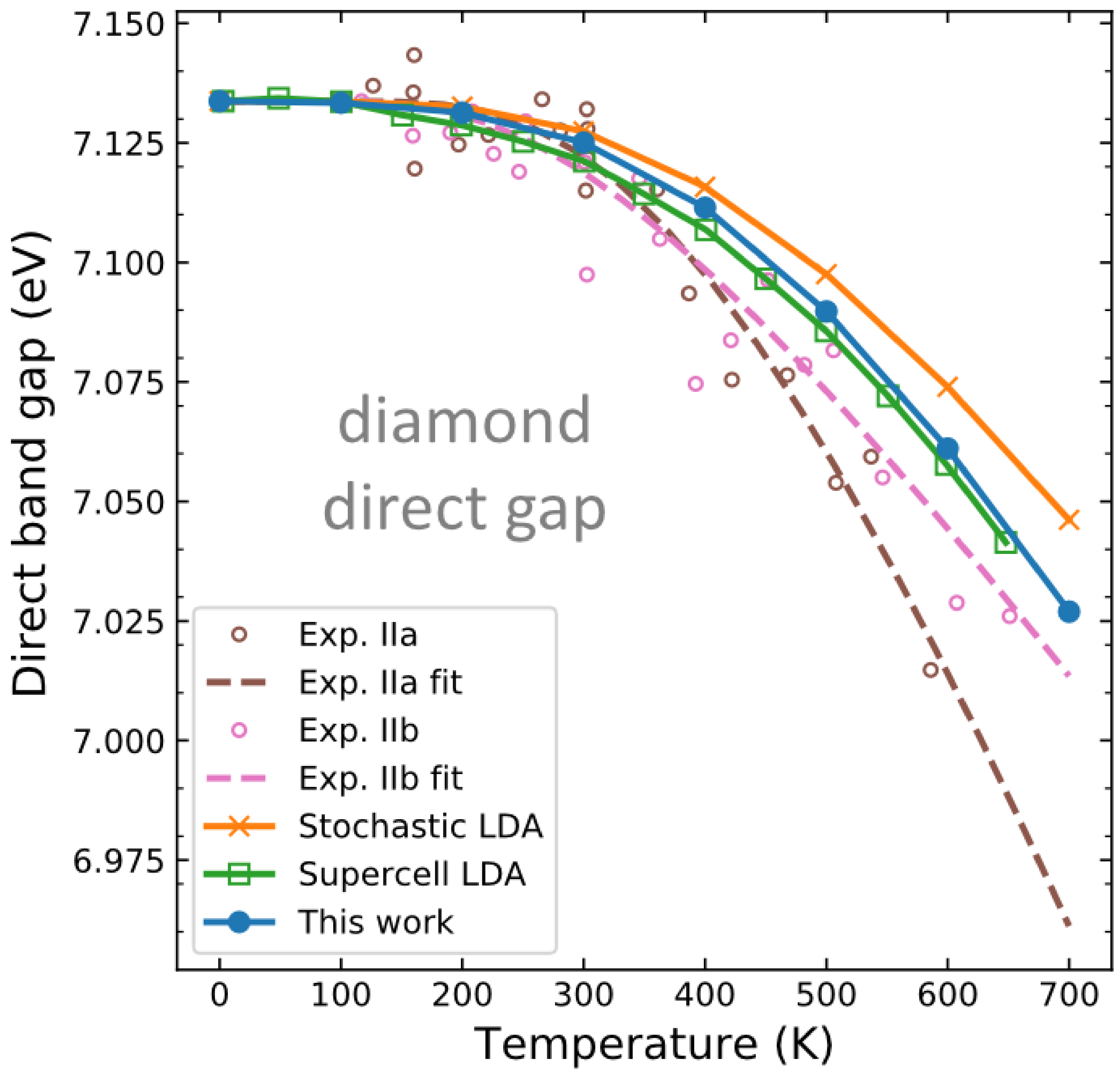

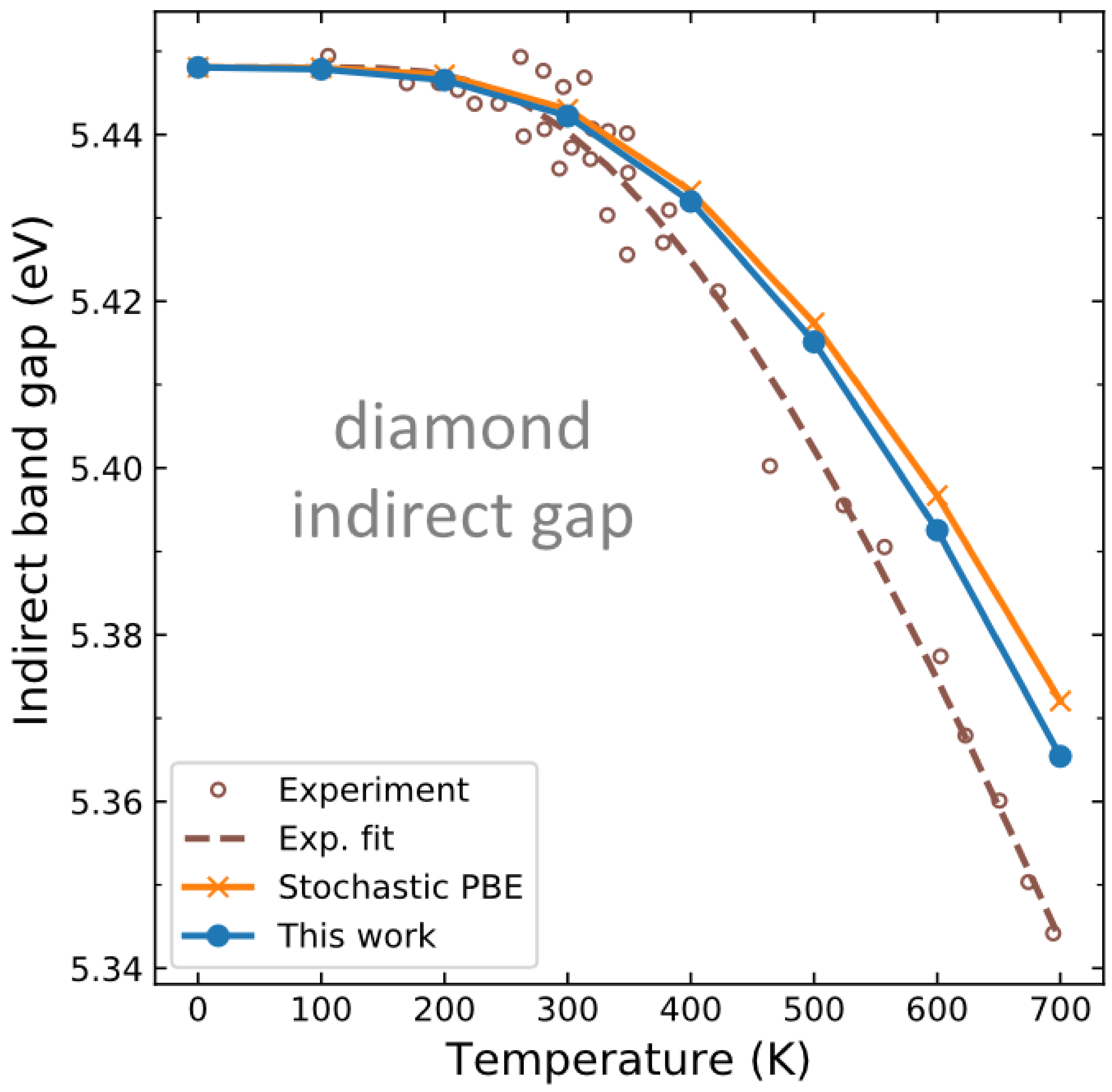

M. Engel, M. Marsman, C. Franchini, and G. Kresse, Phys. Rev. B 101, 184302 (2020)

PAW Method

Projector-augmented-wave (PAW) method in VASP

- Fast
- Accurate
- Robust

PAW advantages extend to electron-phonon coupling:

- ZPR converges fast with **pseudo (PS)** approach
- **All-electron (AE)** approach available for other observables

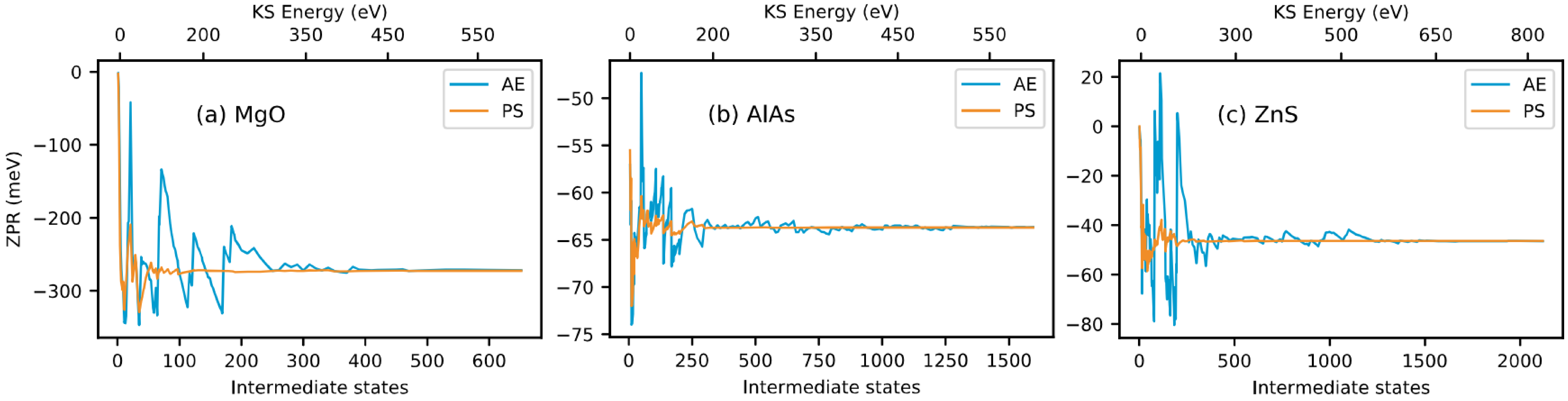

L. Chaput, A. Togo, and I. Tanaka, Phys. Rev. B 100, 174304 (2019)

M. Engel, M. Marsman, C. Franchini, and G. Kresse, Phys. Rev. B 101, 184302 (2020)

M. Engel, H. Miranda, L. Chaput, *et al.*, Phys. Rev. B 106, 094316 (2022)

ZPR Performance

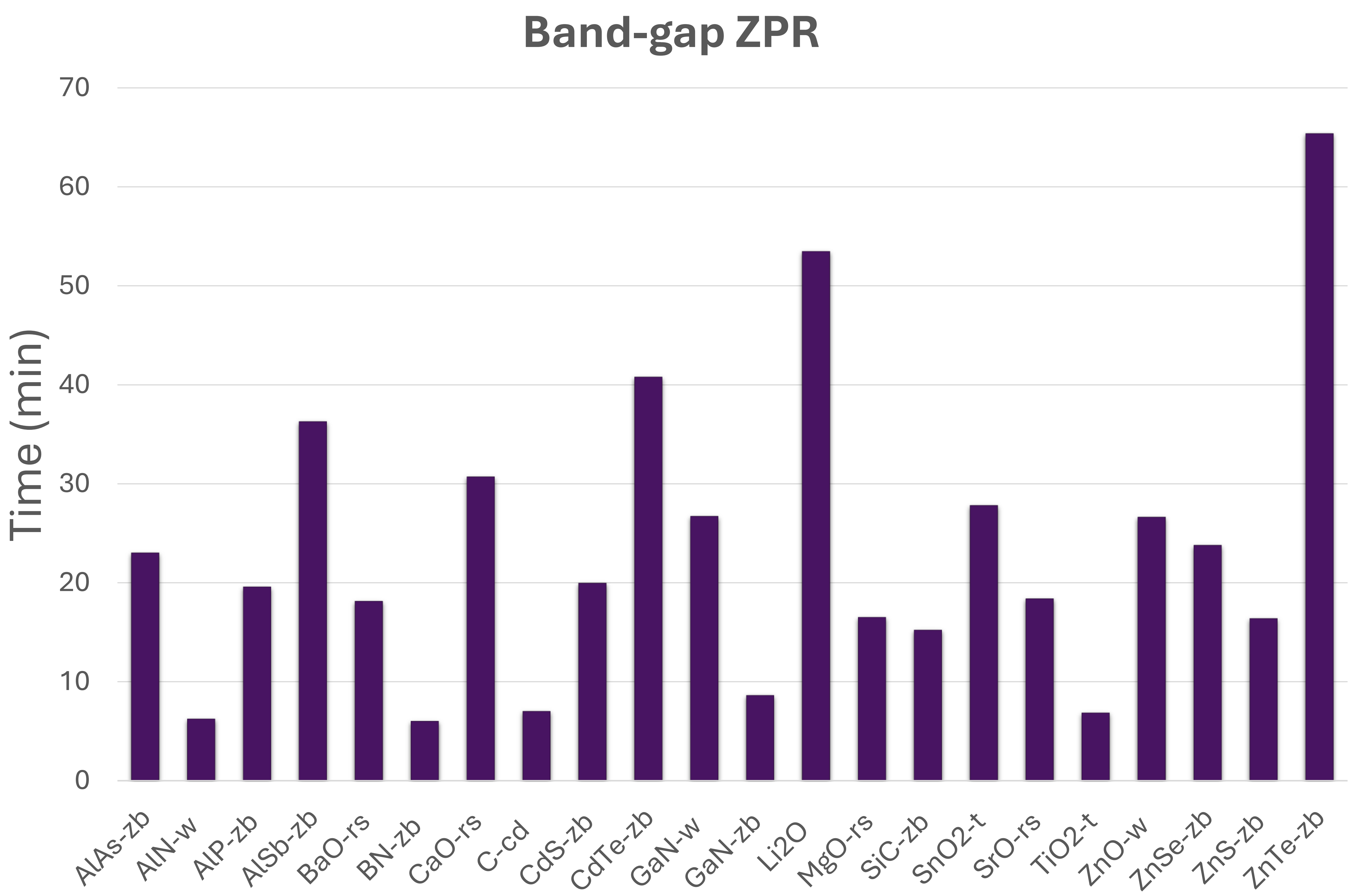

On average per calculation:

- 520 bands
- 230000 k-points
- 128 CPU cores
- 24 minutes

Total ~8.5 hours
One machine, one workday

Transport Properties

$\sigma \equiv \mathcal{L}^{(0)}$ Electrical conductivity

$\Pi \equiv \frac{1}{e}\frac{\mathcal{L}^{(1)}}{\mathcal{L}^{(0)}}$ Peltier coefficient

$S \equiv \frac{1}{eT}\frac{\mathcal{L}^{(1)}}{\mathcal{L}^{(0)}}$ Seebeck coefficient

$k_e \equiv \frac{1}{e^2 T}\left[\frac{\left(\mathcal{L}^{(1)}\right)^2}{\mathcal{L}^{(0)}} - \mathcal{L}^{(2)}\right]$ Charge-carrier contribution to thermal conductivity

Obtained from the generalized transport coefficients, $\mathcal{L}_{\alpha\beta}^{(m)}$:

$$\mathcal{L}_{\alpha\beta}^{(m)}(T) = -\int_{-\infty}^{\infty} d\epsilon\, \mathcal{T}_{\alpha\beta}(\epsilon, T)(\epsilon - \epsilon_F)^m \frac{\partial f(\epsilon - \epsilon_F, T)}{\partial \epsilon}$$

$$\mathcal{T}_{\alpha\beta}(\epsilon, T) = e^2 \sum_n \int \frac{d\mathbf{k}}{\Omega_{\mathrm{BZ}}} v_{n\mathbf{k}\alpha} v_{n\mathbf{k}\beta} \tau_{n\mathbf{k}}(T) \delta(\epsilon - \epsilon_{n\mathbf{k}})$$

Relaxation time, $\tau_{n\mathbf{k}}$, can be obtained from electron self-energy

Electron Mobility in GaAs

GaAs requires very dense k-point meshes to converge
However: We can choose only a small energy window around chemical potential to calculate mobilities

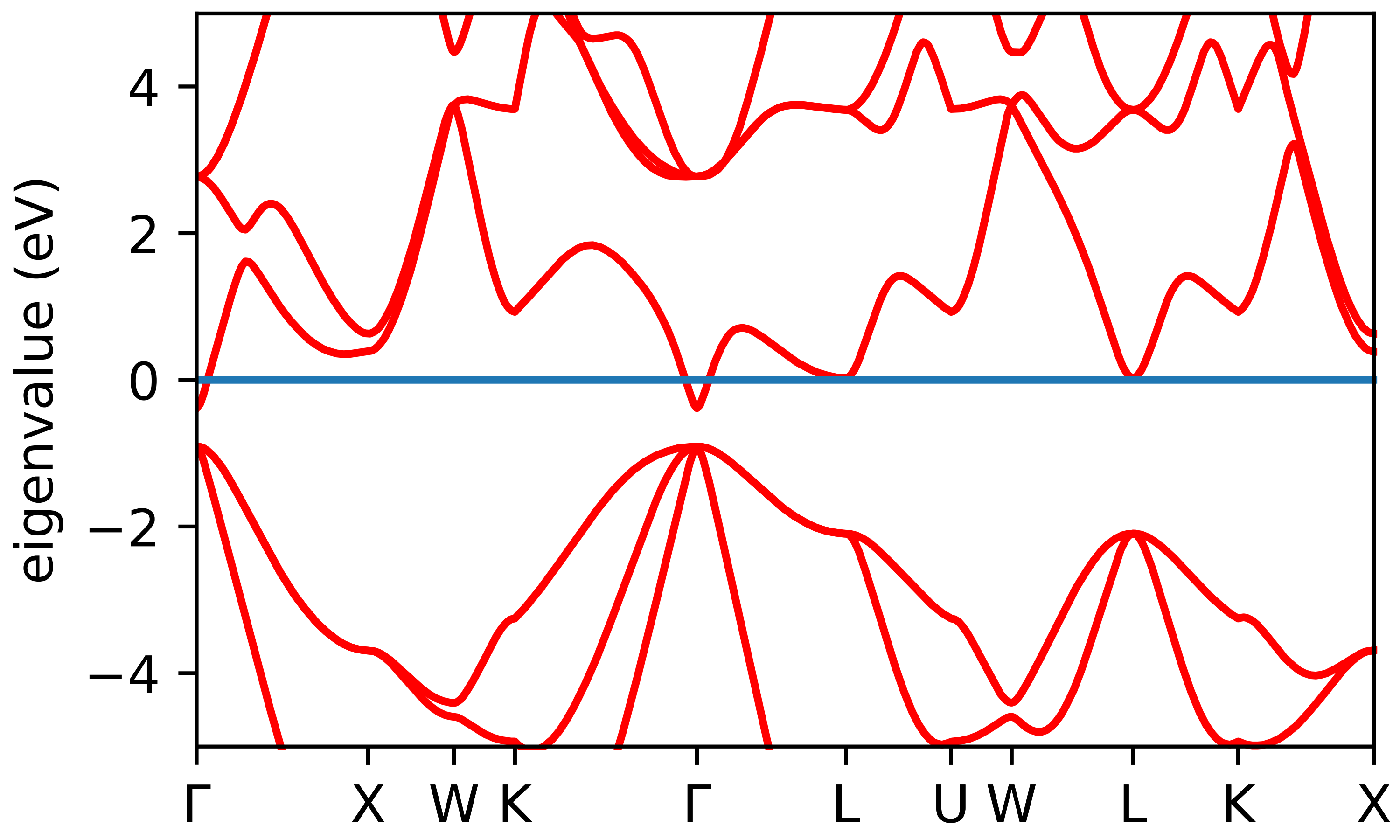

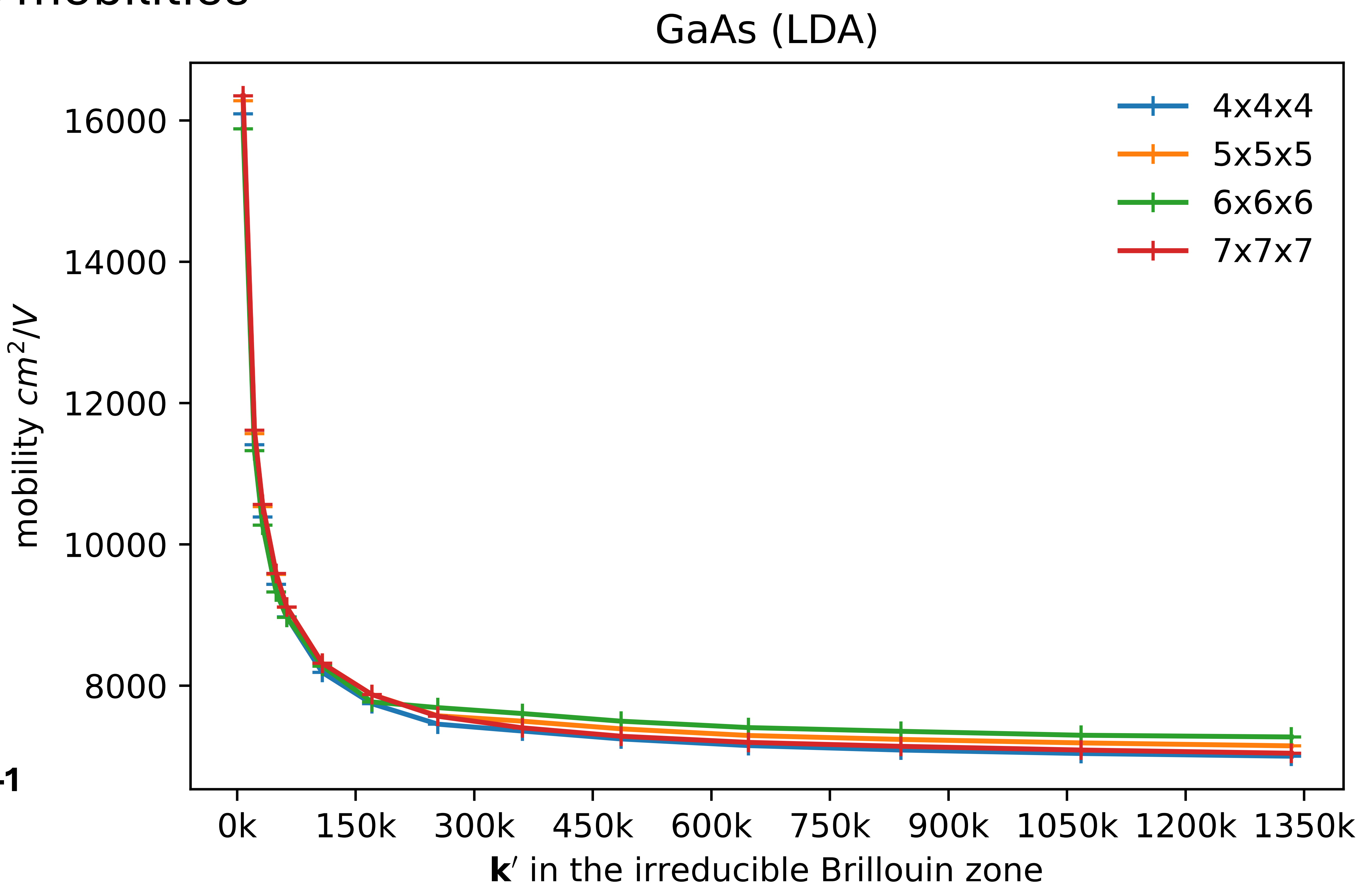

VASP: **7045 $cm^2V^{-1}s^{-1}$**
Exp. between **7000** and **12000 $cm^2V^{-1}s^{-1}$**

G. Brunin, H. P. C. Miranda, M. Giantomassi, *et al.*, Phys. Rev. B 102, 094308 (2020)

Features - Overview

Included in the upcoming release

- Electron self-energy
  - Renormalization of the electronic band structure
  - Band-gap renormalization
  - Electron lifetimes or linewidths
  - Electronic transport properties
- Spin-orbit coupling
- Efficient parallelization
  - Over bands (with memory distribution option)
  - Over k-points
- HDF5 + py4vasp support
- Flexible input via accumulators

Coming in a future update

- Phonon self-energy
- Superconductivity
- GPU support
- Wannier interpolation
- metaGGA and hybrids
- …

VASP: Present and Future

Manuel Engel, Martijn Marsman, and Georg Kresse

universität wien

Outline

Total energies

Electronic structure

Machine learned force fields

Outlook

Vienna *Ab initio* Simulation Package (VASP)

Electronic structure from first principles:

$$\hat{H}\Psi(\mathbf{r}_1, \ldots, \mathbf{r}_N) = E\Psi(\mathbf{r}_1, \ldots, \mathbf{r}_N)$$

Approximations:

- Density Functional Theory (DFT)
- Hartree-Fock/DFT-HF hybrid functionals
- RPA: ACFDT and *GW*
- BSE

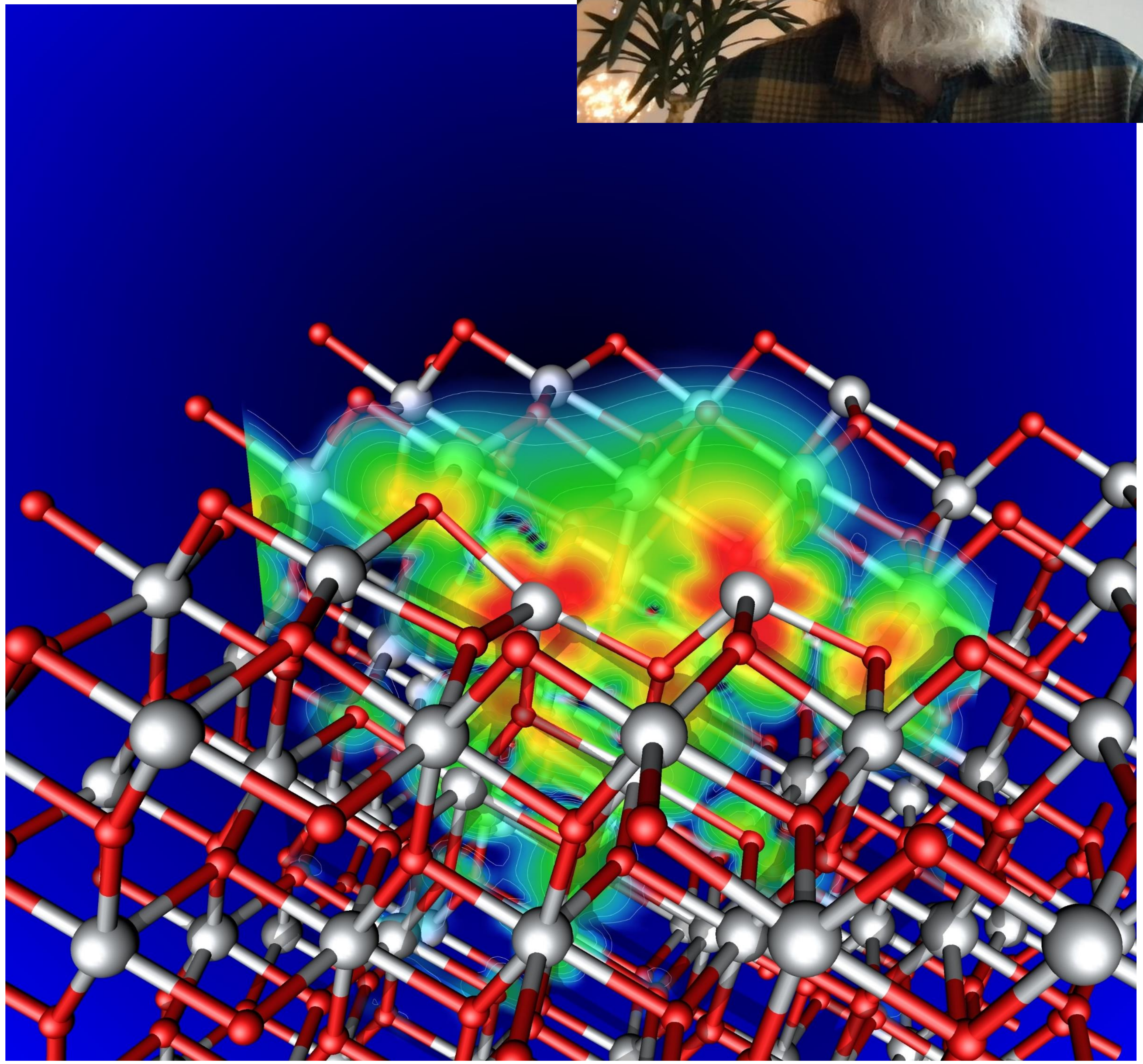

- 3500+ licensed academic and industrial groups worldwide
- 13k+ publications in 2023 and 2nd most used atomistic simulation software (10.5281/zenodo.10894860)
- Developed in the group of Prof. G. Kresse at the University Vienna and the VASP Software GmbH

Catalysis: dehydrogenation of propane in Mordenite results

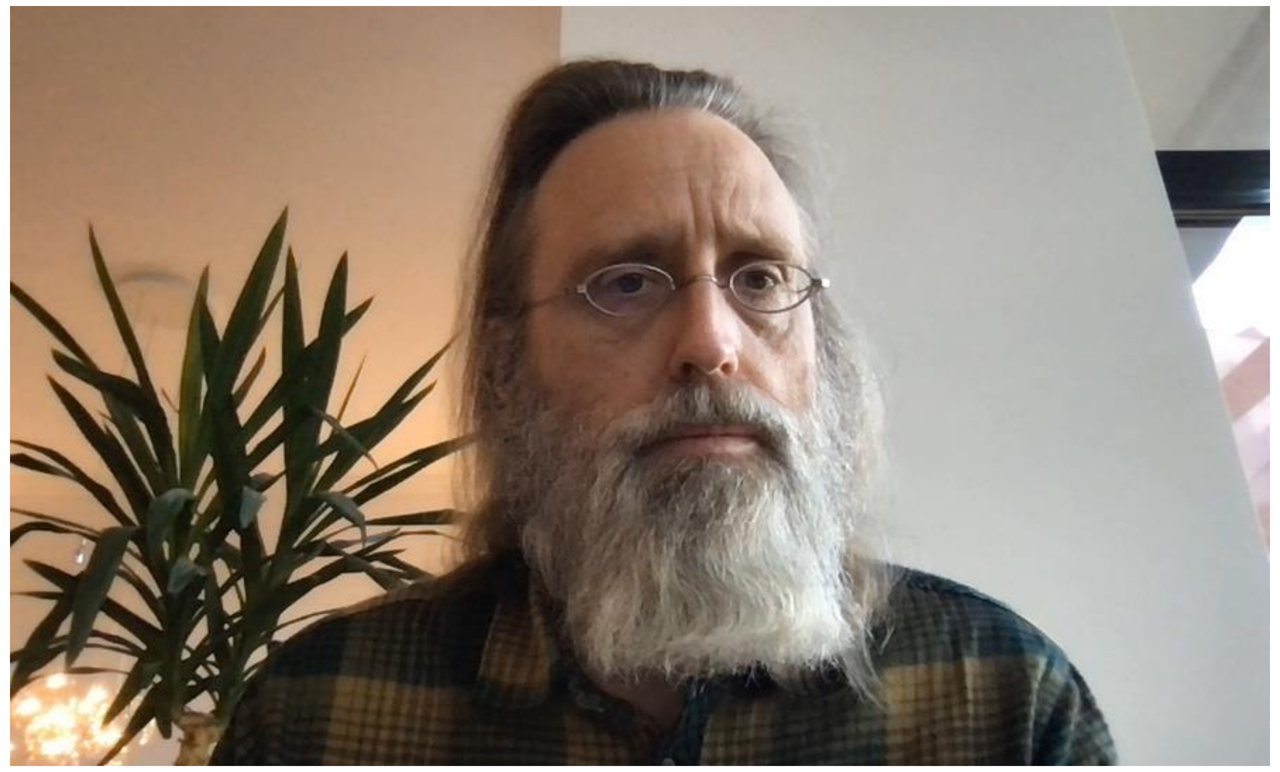

$$\mathrm{MOR{-}Zn} + C_3H_8 \rightarrow \mathrm{MOR{-}Zn} \cdots C_3H_8,$$
$$\mathrm{MOR{-}Zn} \cdots C_3H_8 \rightarrow \mathrm{H{-}MOR{-}Zn{-}}C_3H_7,$$
$$\mathrm{H{-}MOR{-}Zn{-}}C_3H_7 \rightarrow \mathrm{MOR{-}Zn} \cdots C_3H_6 + H_2$$
$$\mathrm{MOR{-}Zn} \cdots C_3H_6 \rightarrow \mathrm{MOR{-}Zn} + C_3H_6.$$

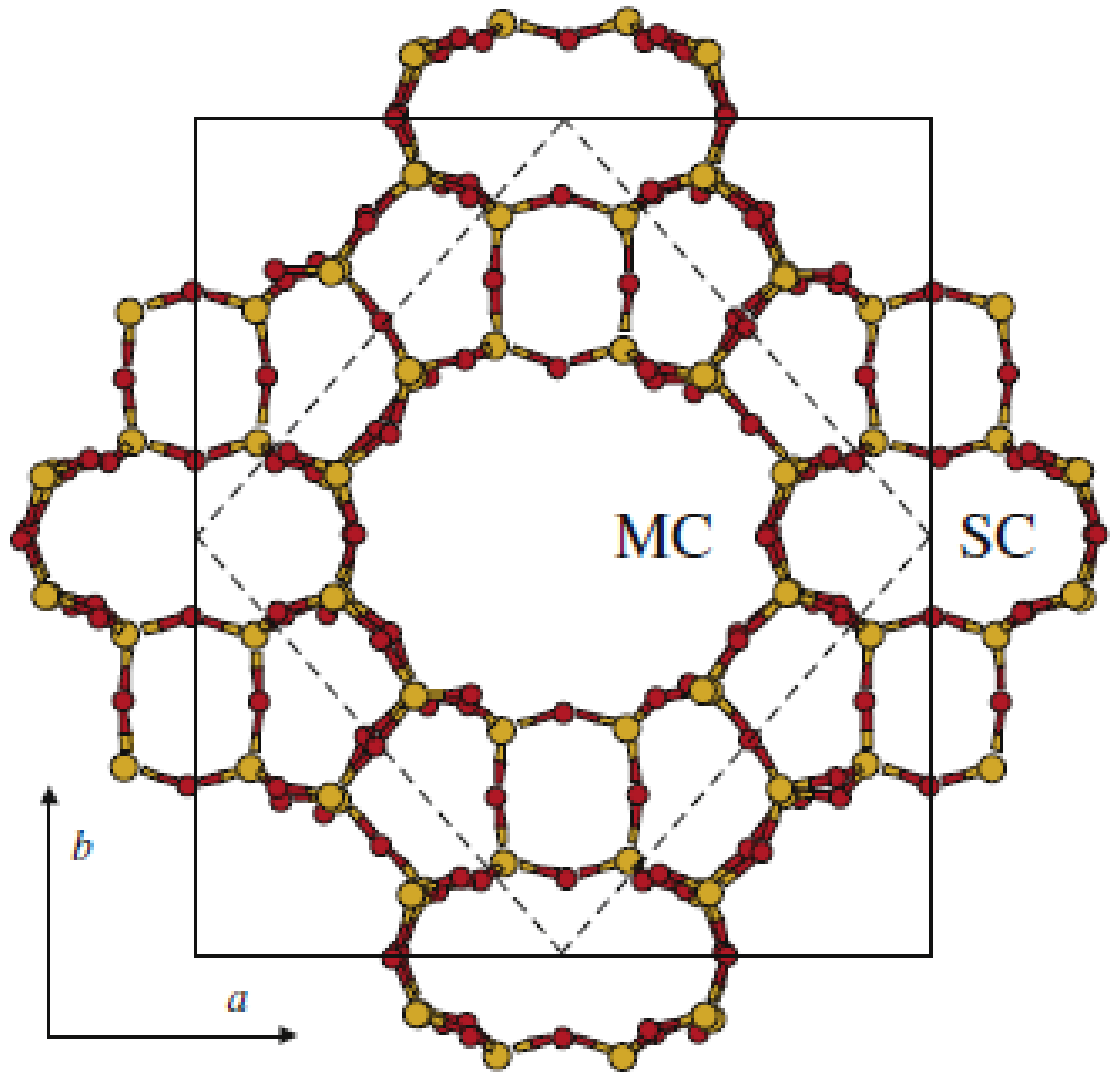

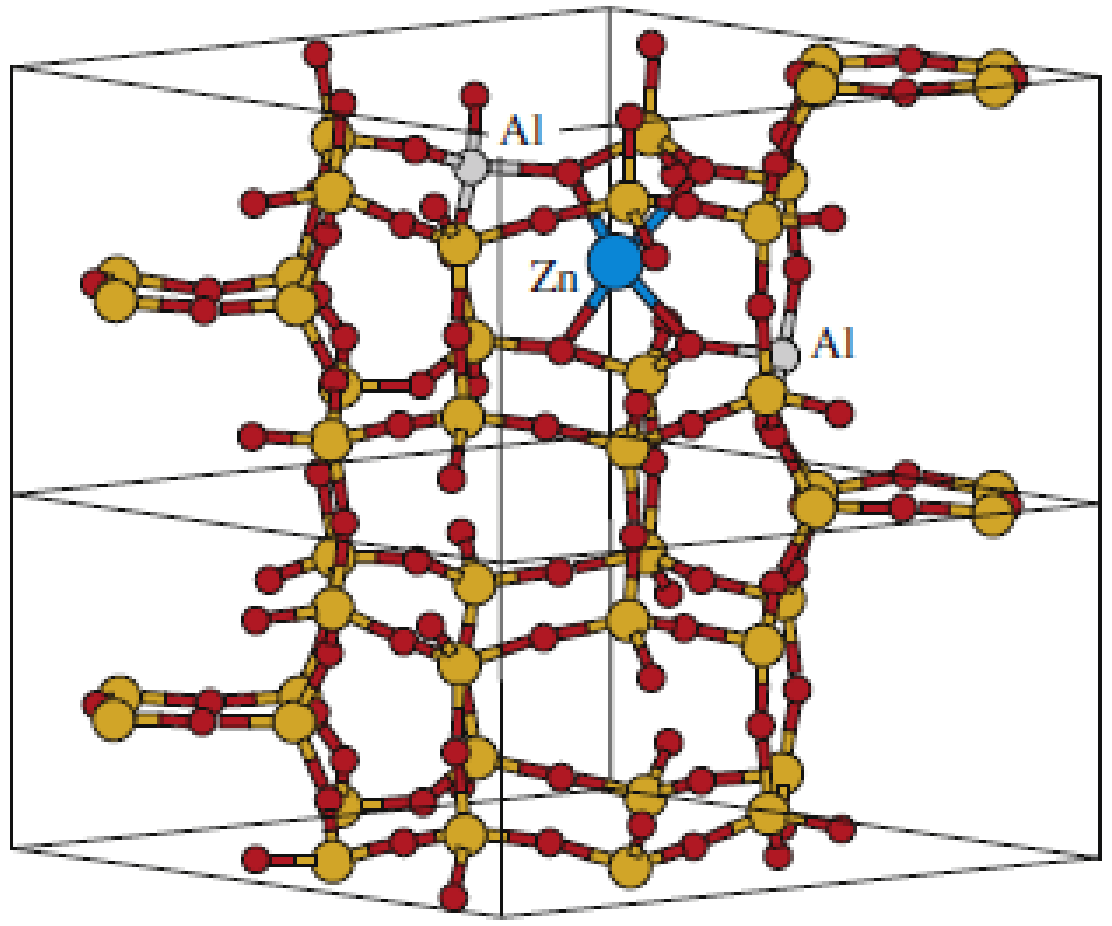

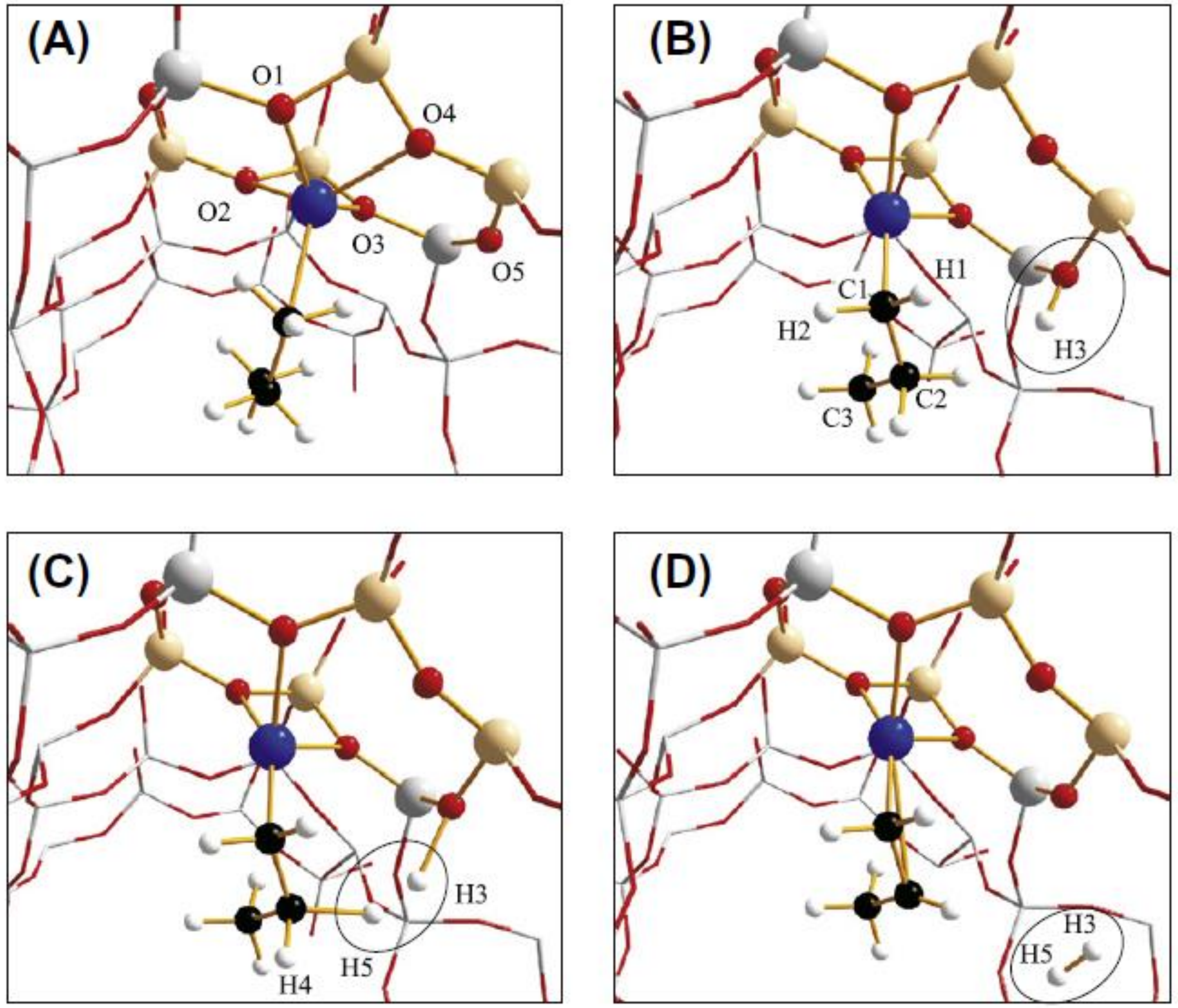

L. Benco et al. / Journal of Catalysis 277 (2011) 104–116

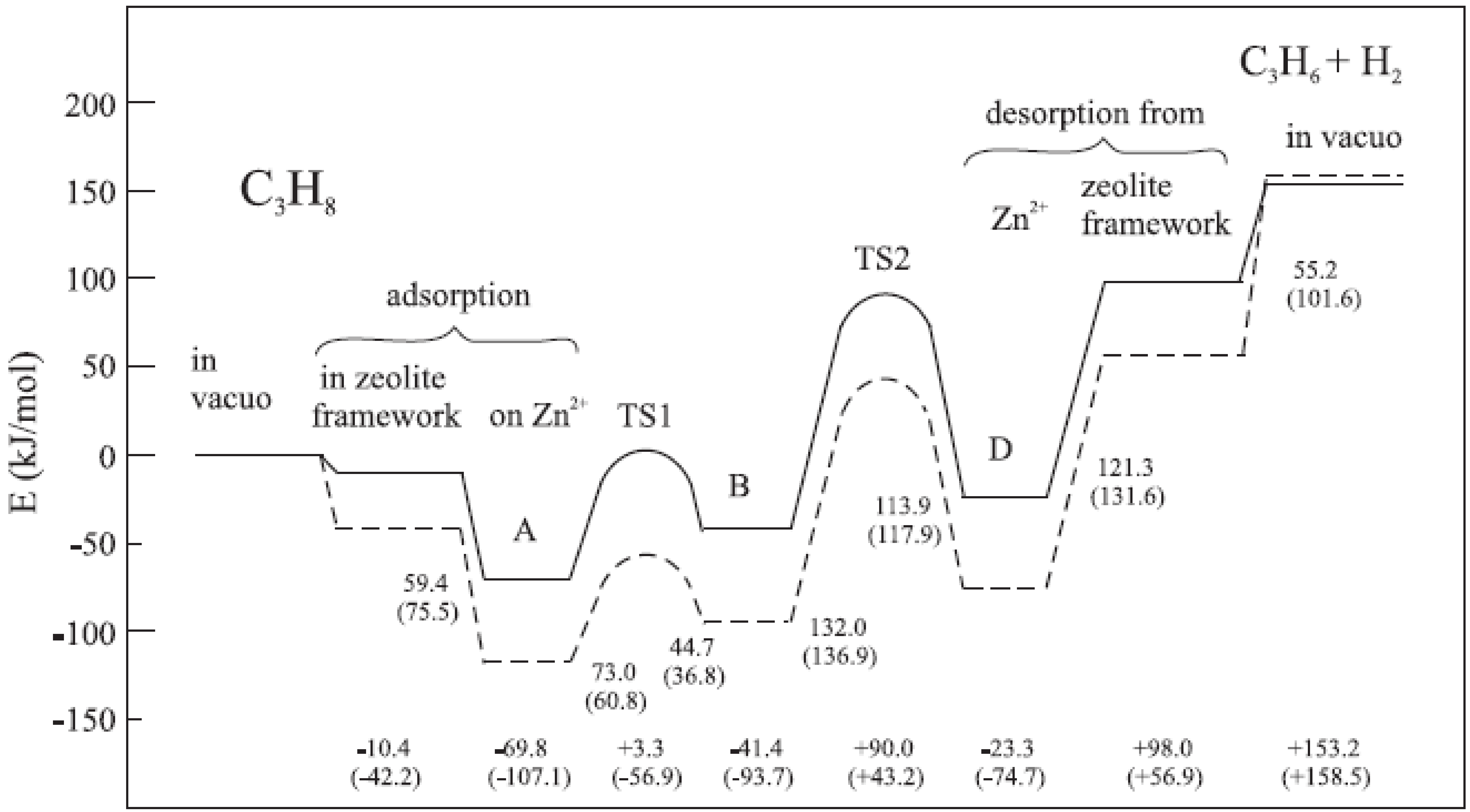
E (kJ/mol)
200
150
100
50
0
-50
-100
-150
C3H8
$C_3H_6 + H_2$
in vacuo
adsorption
in zeolite framework
on Zn2+
TS1
A
B
TS2
D
desorption from
Zn2+
zeolite framework
in vacuo
59.4 (75.5)
73.0 (60.8)
44.7 (36.8)
132.0 (136.9)
113.9 (117.9)
121.3 (131.6)
55.2 (101.6)
-10.4 (-42.2)
-69.8 (-107.1)
+3.3 (-56.9)
-41.4 (-93.7)
+90.0 (+43.2)
-23.3 (-74.7)
+98.0 (+56.9)
+153.2 (+158.5)

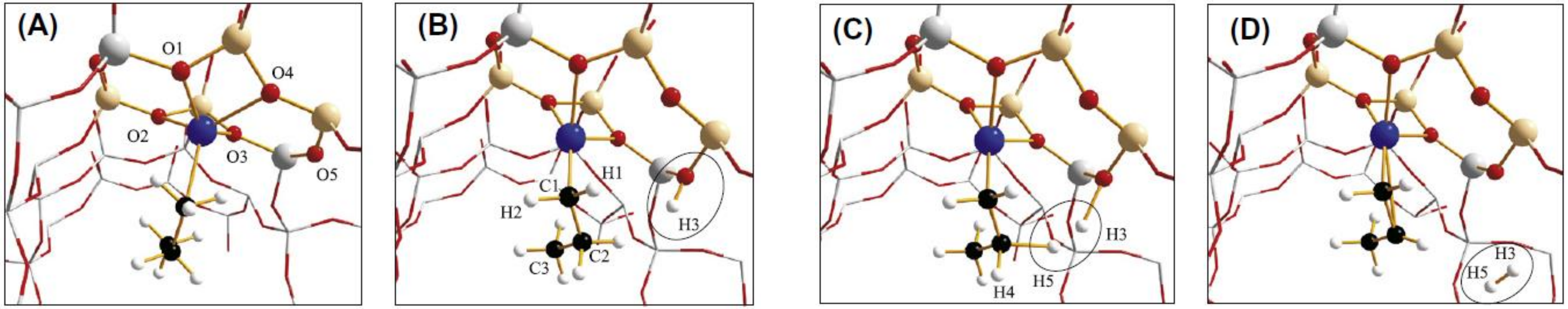
(A)
O1
O4
O2
O3
O5
(B)
C1
H1
H2
C2
C3
H3
(C)
H3
H5
H4
(D)
H3
H5

RPA: CO @ *d*-metal (111)-surfaces

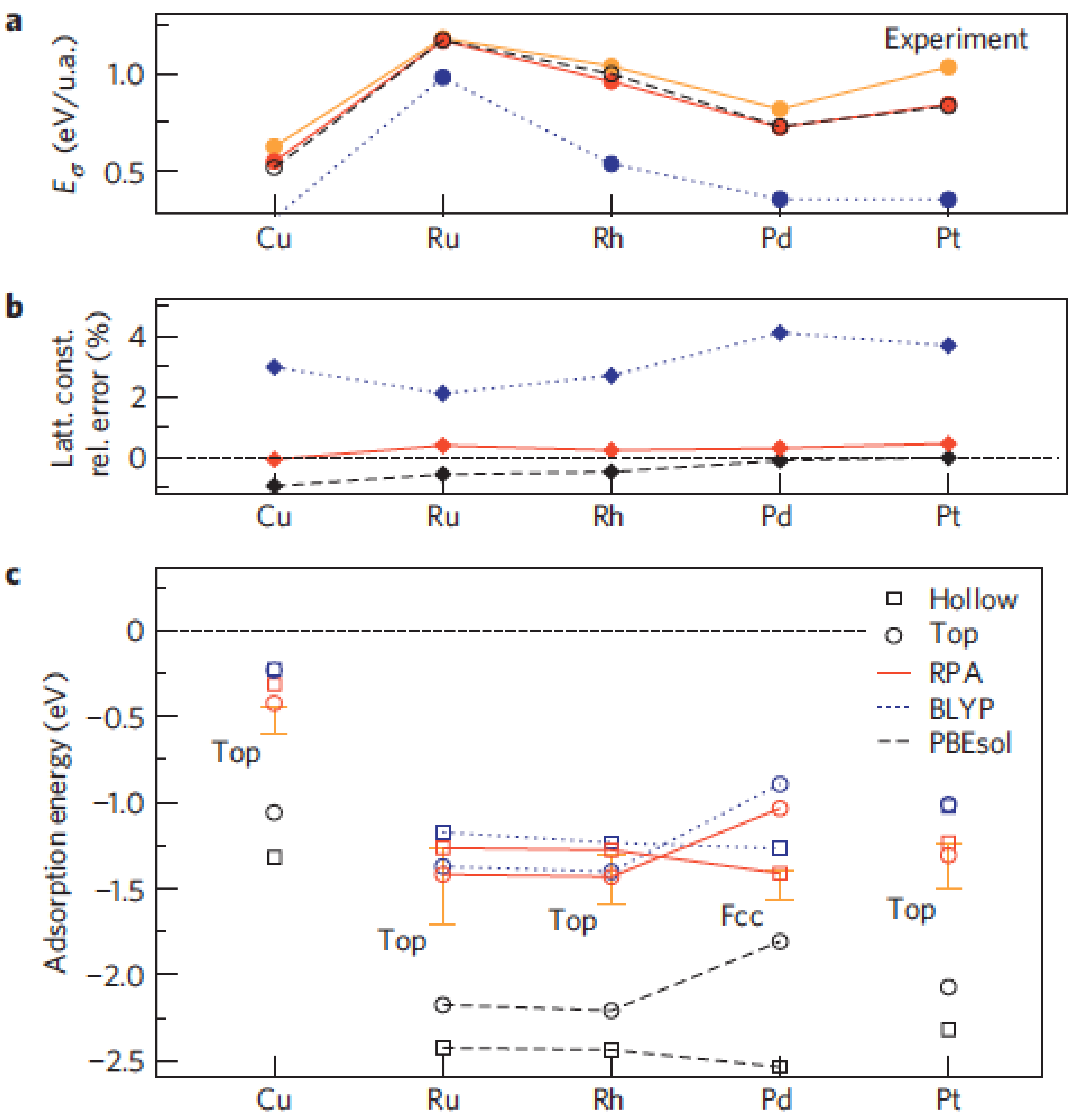

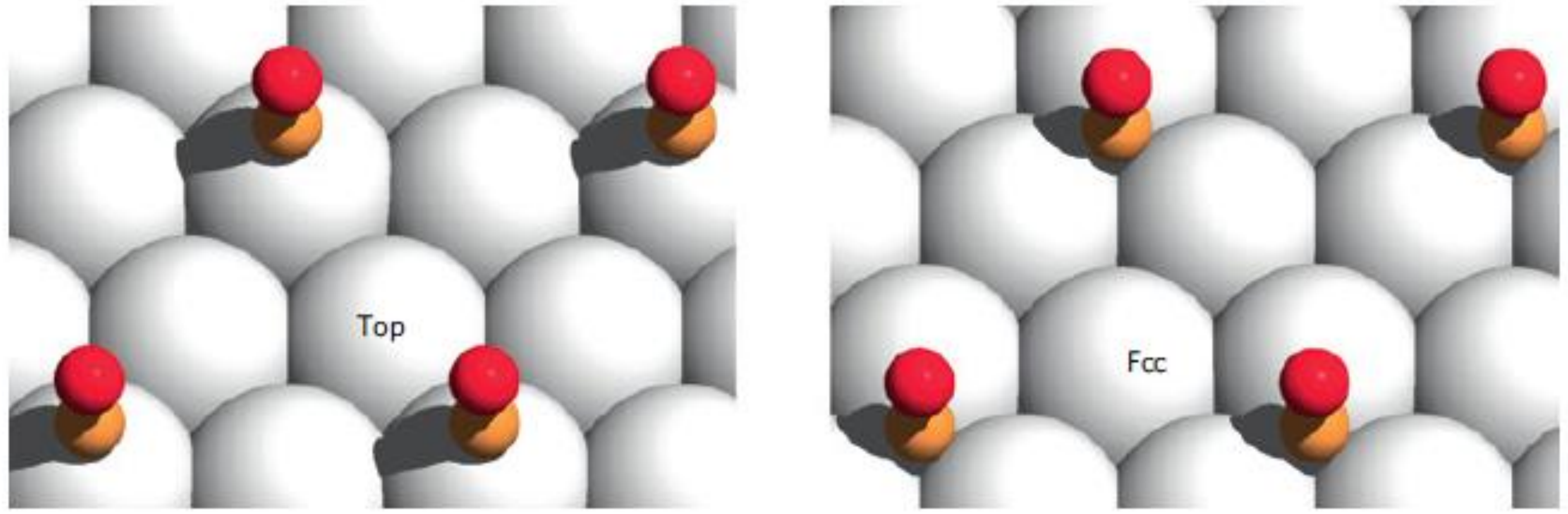

Figure 3 | Surface energies, lattice constants and adsorption energies. **a**, Fcc(111) surface energies (E_σ) for PBEsol, BLYP and RPA. Experimental surface energies are deduced from liquid-metal data[24,25]. **b**, Lattice constants for PBEsol, RPA and BLYP. **c**, Adsorption energies for the atop and hollow sites of CO on Cu, late 4*d* metals and Pt for PBEsol, RPA and BLYP. Experimental data with error bars are from ref. 26. The error bars correspond to the spread of the experimental results.

Schimka et al., Nature Materials 9, 741 (2010)

RPA: CO @ *d*-metal (111)-surfaces

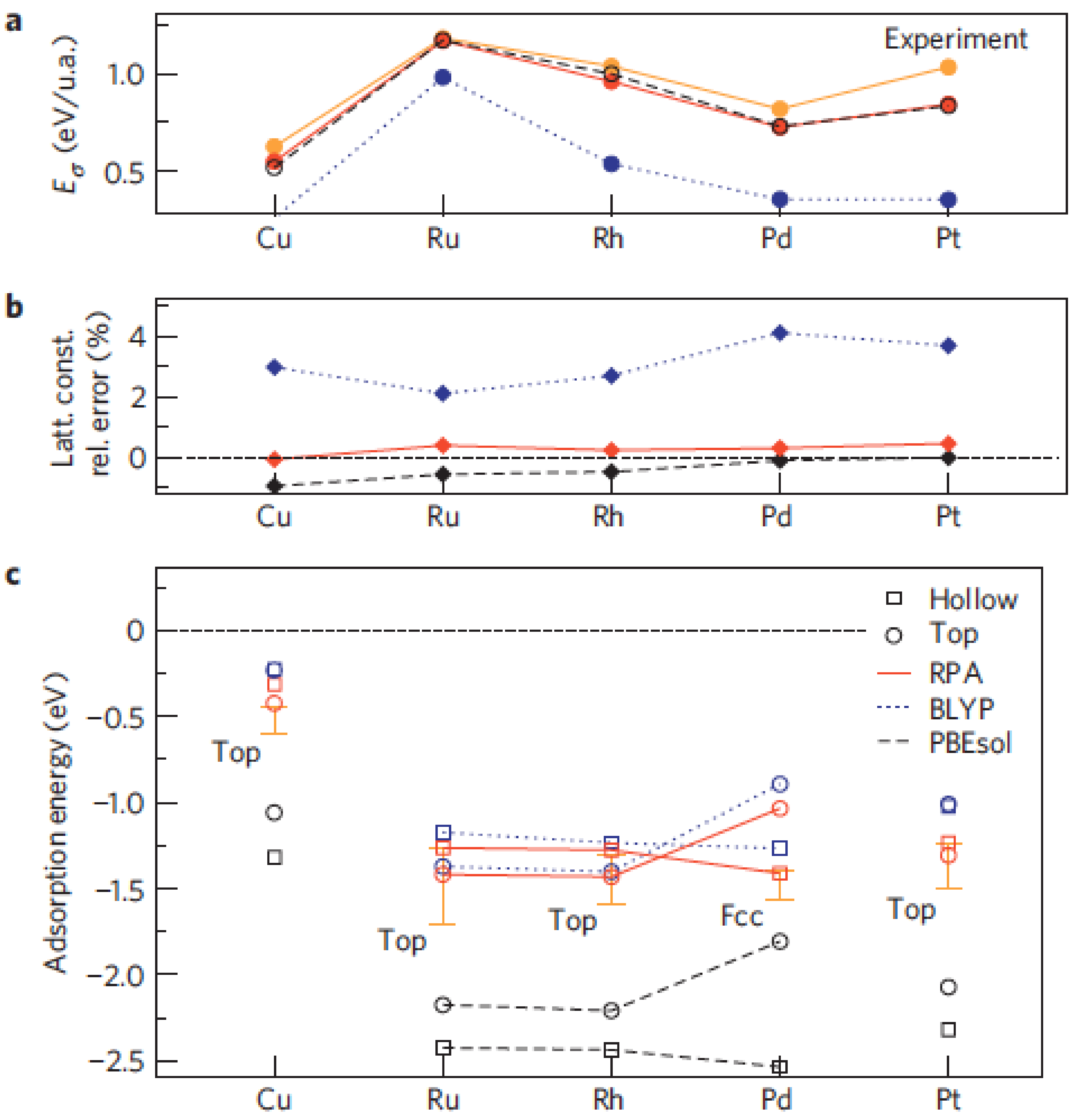

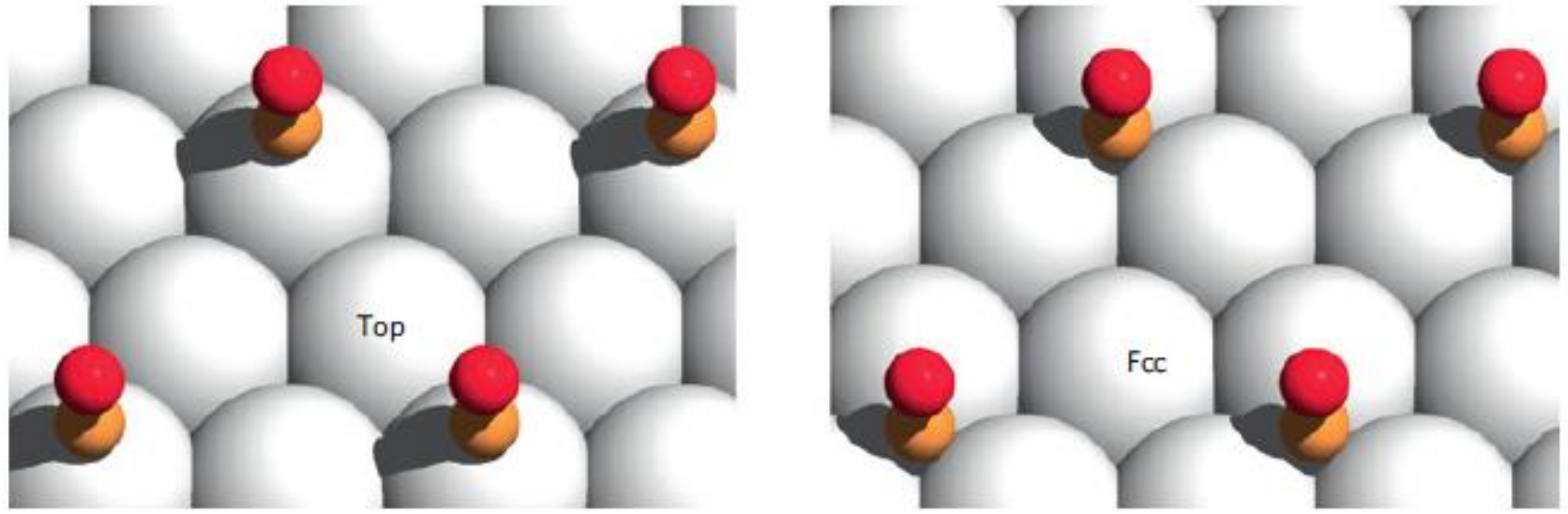

- Right site preference
- Good adsorption energies
- Excellent lattice constants
- Good surface energies

One-electron/Quasi-particle picture

DFT: Kohn-Sham eq.

$$\left(-\frac{1}{2}\Delta + V_{\mathrm{ext}}(\mathbf{r}) + V_{\mathrm{H}}(\mathbf{r}) + V_{\mathrm{xc}}\left[\rho\right](\mathbf{r})\right)\psi_{n\mathbf{k}}(\mathbf{r}) = \epsilon_{n\mathbf{k}}\psi_{n\mathbf{k}}(\mathbf{r})$$

DFT-HF hybrid functionals: Roothaan eq.

$$\left(-\frac{1}{2}\Delta + V_{\mathrm{ext}}(\mathbf{r}) + V_{\mathrm{H}}(\mathbf{r})\right)\psi_{n\mathbf{k}}(\mathbf{r}) + \int V_{\mathrm{X}}\left[\{\psi_o\}\right](\mathbf{r},\mathbf{r}')\psi_{n\mathbf{k}}(\mathbf{r}')d\mathbf{r}' = \epsilon_{n\mathbf{k}}\psi_{n\mathbf{k}}(\mathbf{r})$$

GW: quasi-particle eq.

$$\left(-\frac{1}{2}\Delta + V_{\mathrm{ext}}(\mathbf{r}) + V_{\mathrm{H}}(\mathbf{r})\right)\psi_{n\mathbf{k}}(\mathbf{r}) + \int \Sigma\left[\{\psi, E\}\right](\mathbf{r},\mathbf{r}', E_{n\mathbf{k}})\psi_{n\mathbf{k}}(\mathbf{r}')d\mathbf{r}' = E_{n\mathbf{k}}\psi_{n\mathbf{k}}(\mathbf{r})$$

DFT, Hybrids, and G_0W_0 (GW_0)

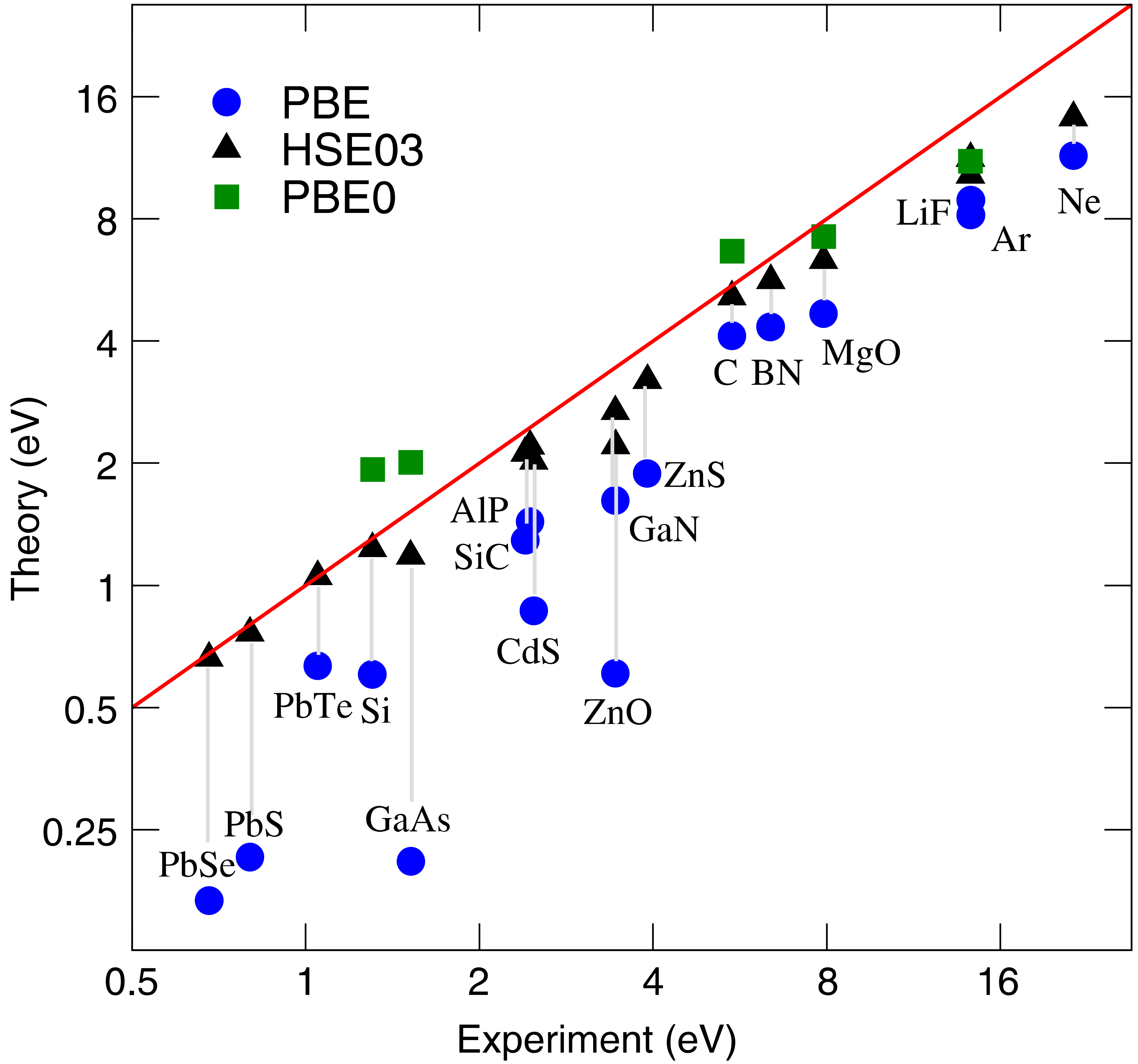

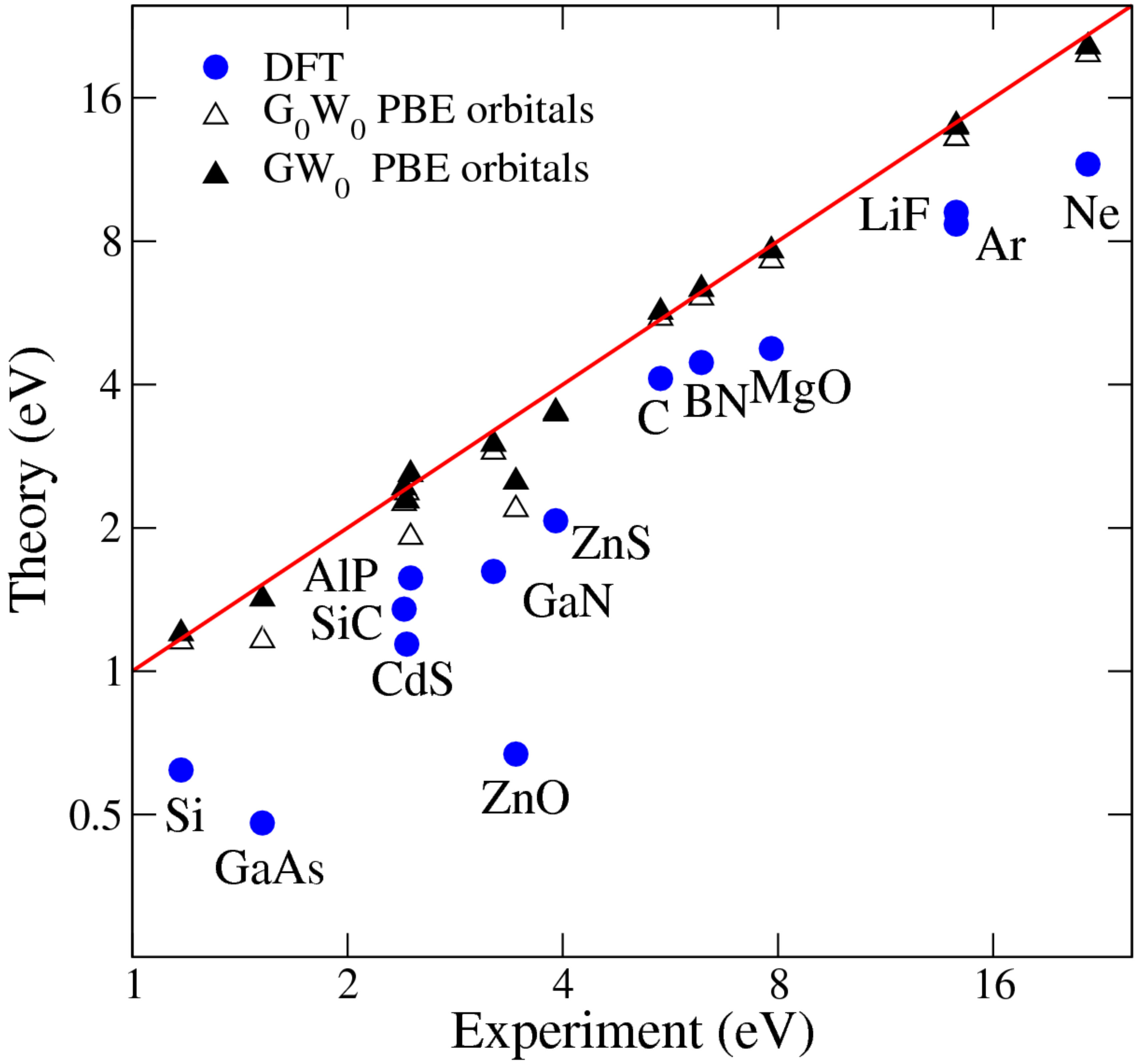

Partially self-consistent GW ($scGW_0$)

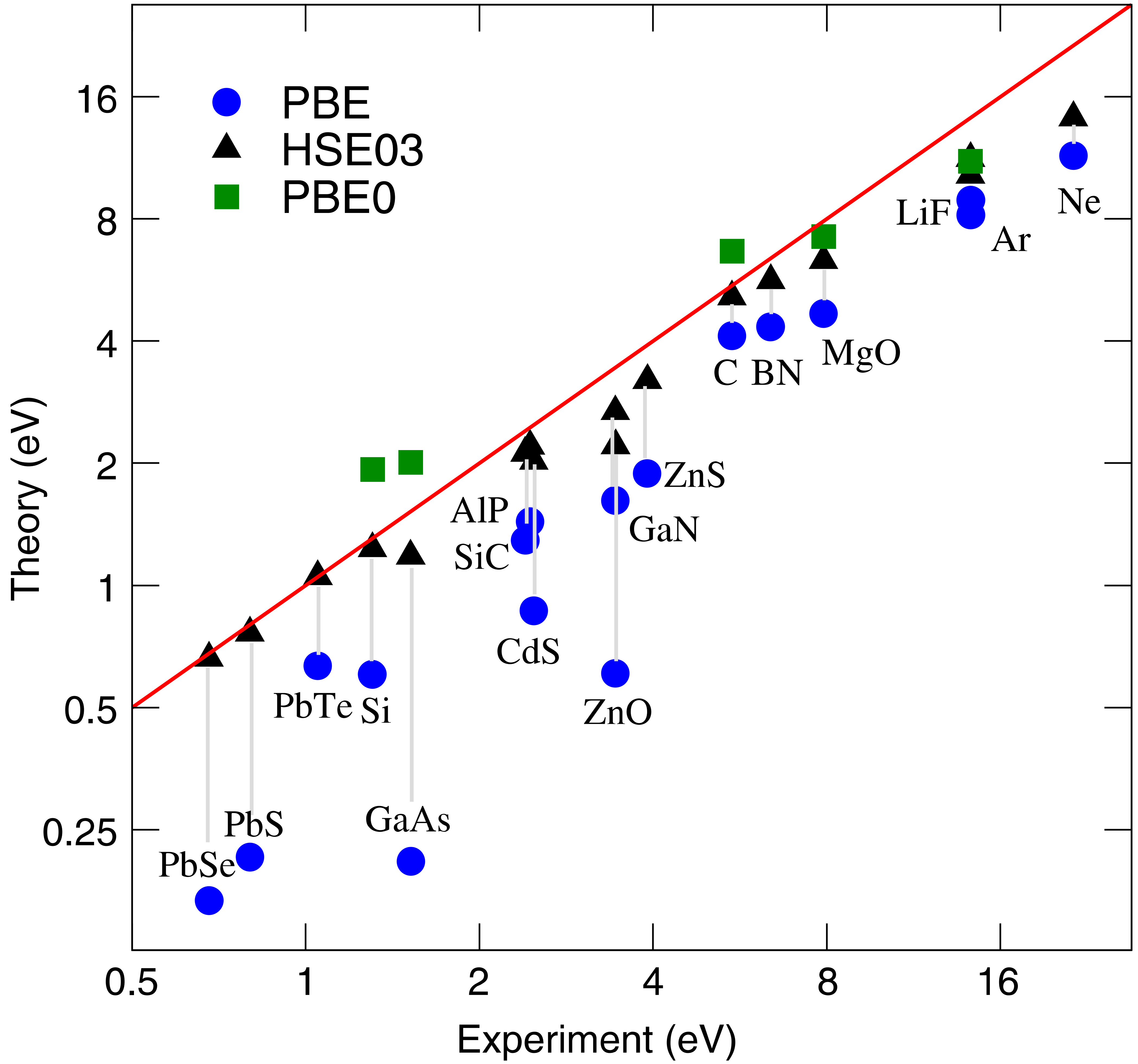

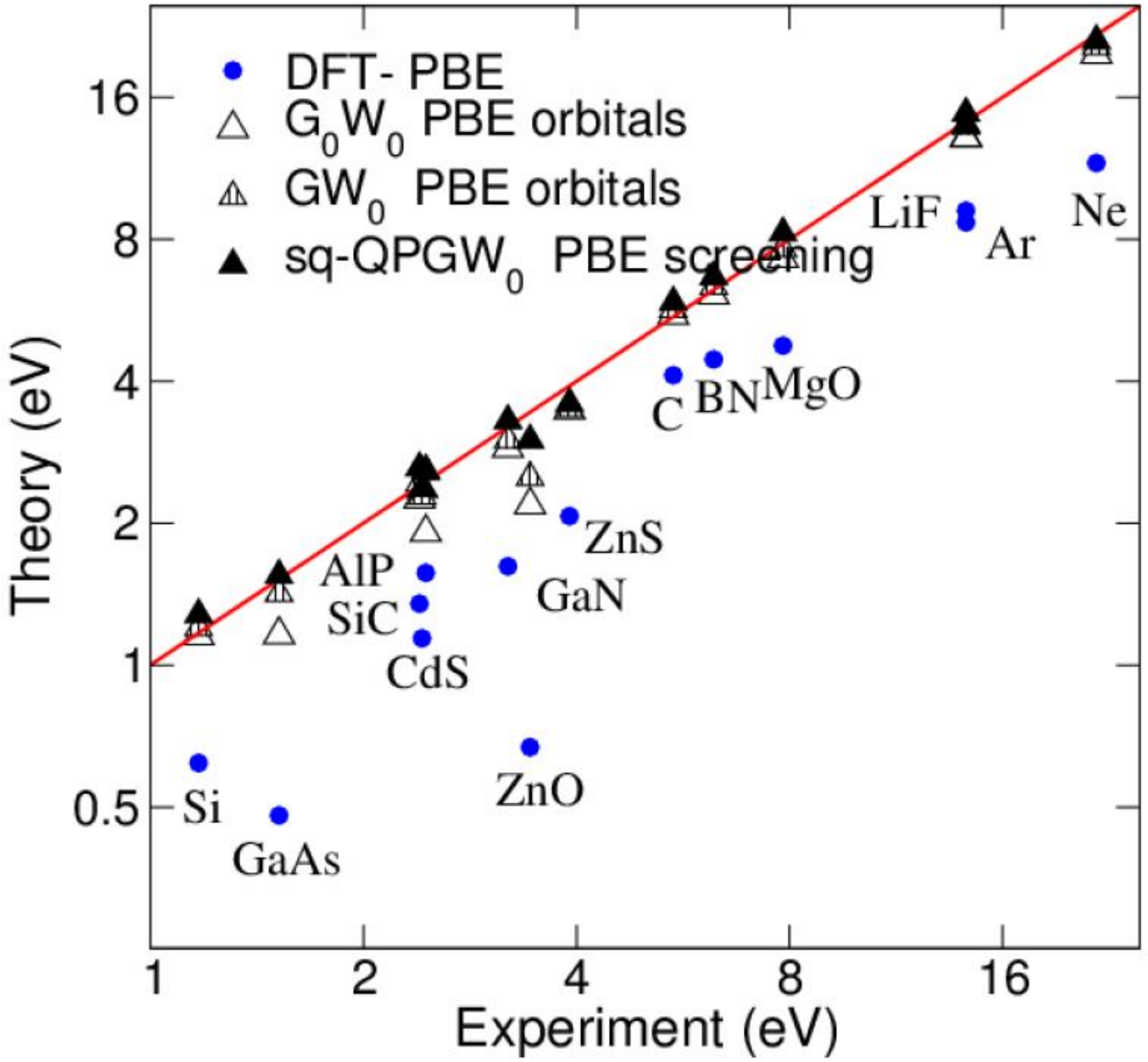

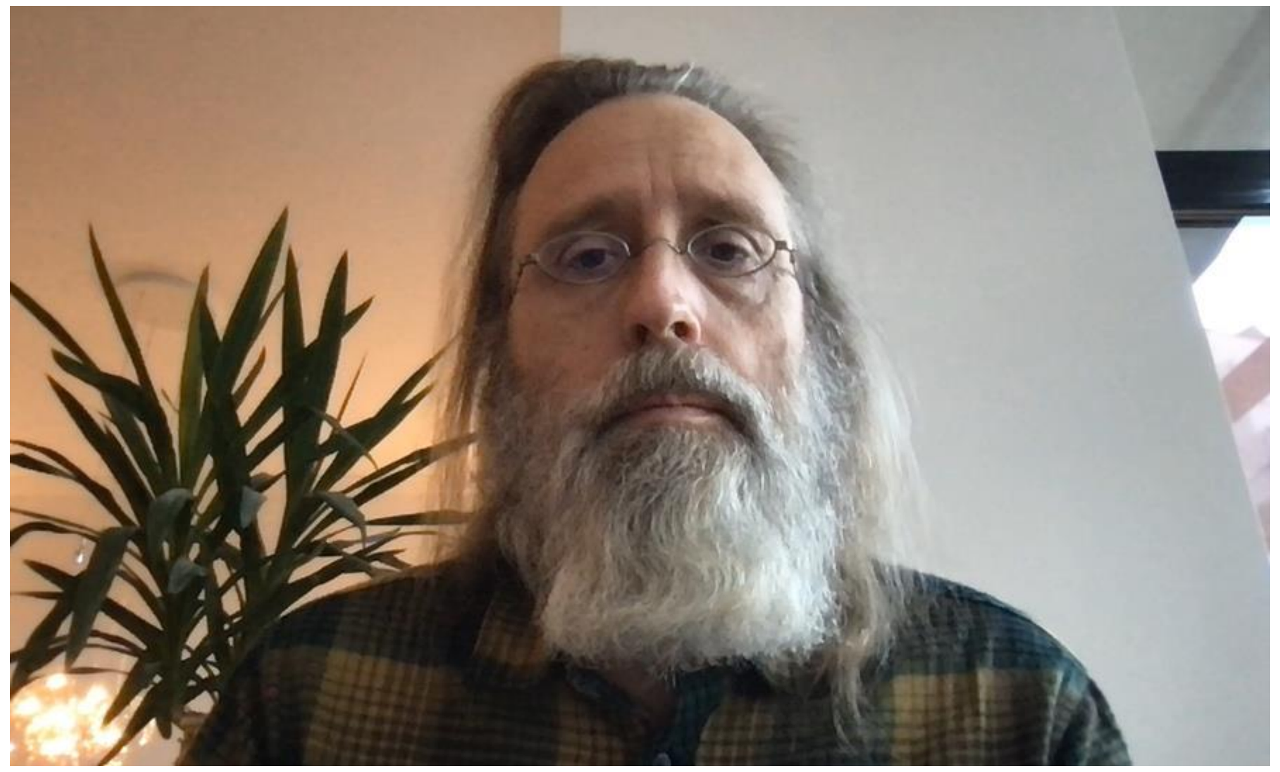

On-the-fly machine learned force fields

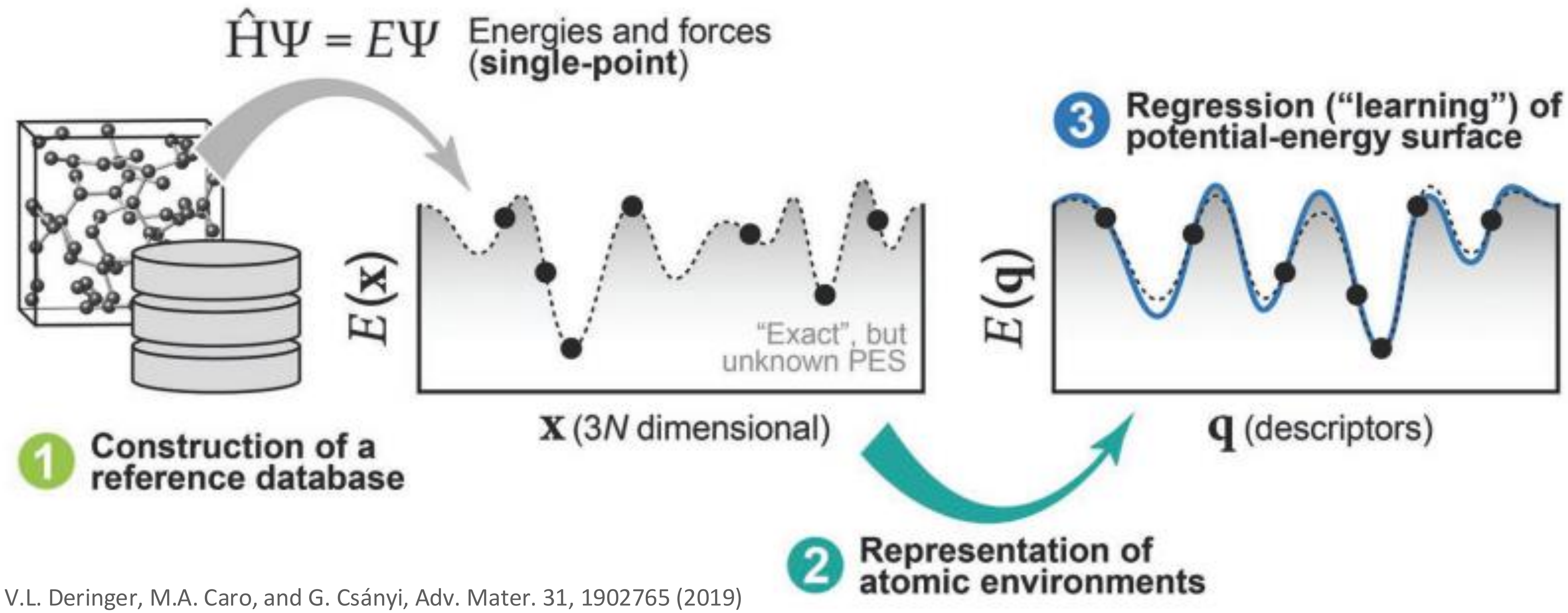

V.L. Deringer, M.A. Caro, and G. Csányi, Adv. Mater. 31, 1902765 (2019)

1. Database of reference calculations
2. Representation of local environments (descriptor, atomic fingerprint)
3. Machine learning algorithm (kernel ridge regression, neural networks)

On-the-fly machine learned force fields

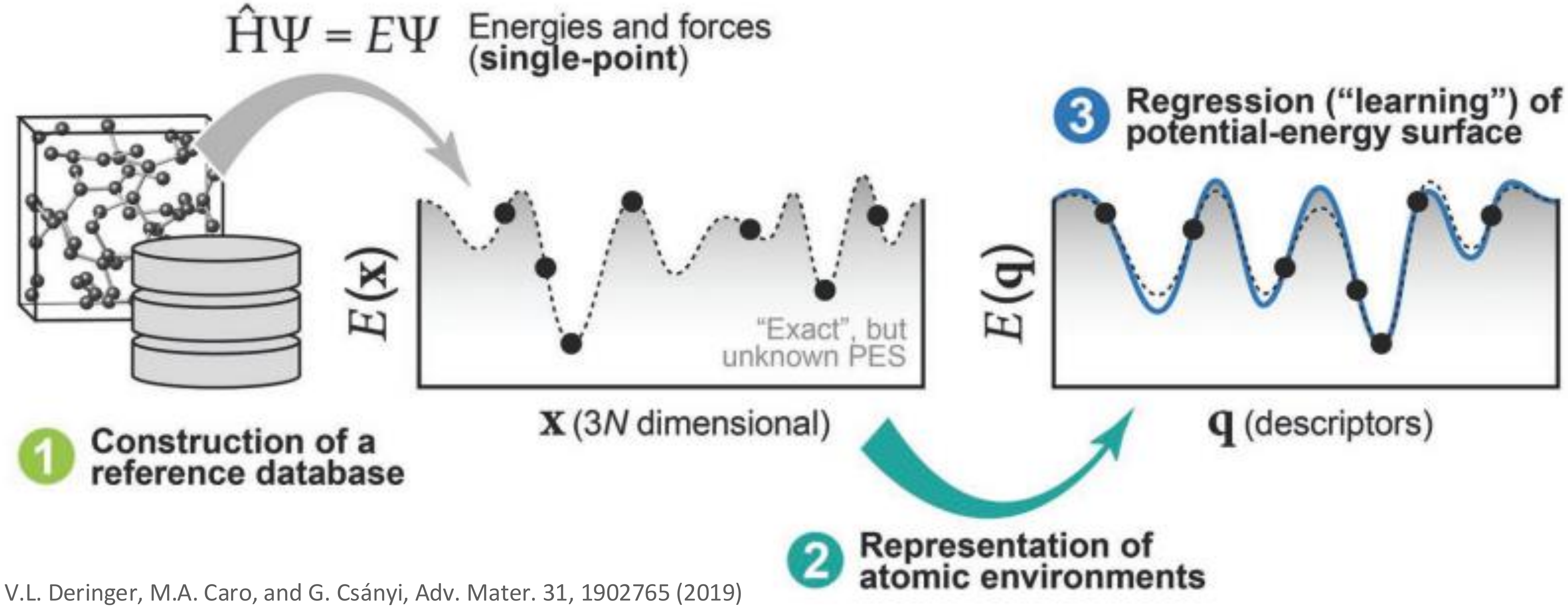

V.L. Deringer, M.A. Caro, and G. Csányi, Adv. Mater. 31, 1902765 (2019)

1. On-the-fly trying during MD runs
2. SOAP descriptor
3. Kernel ridge regression

On-the-fly machine learned force fields

- Manual creation of training database is laborious
- VASP implements an on-the-fly training algorithm
- Can be enabled in regular MD simulation
- Automatically creates and enhances training data
- Automatically selects local reference configurations
- Automatically improves ML force field
- Ideally, after a while no more ab initio calculations are performed and ML prediction is used exclusively
- On-the-fly training requires an estimate of error
- Uses Bayesian variance of atomic forces as a criterion for necessity of ab initio calculation
- Can combine different runs to create a versatile ML force field

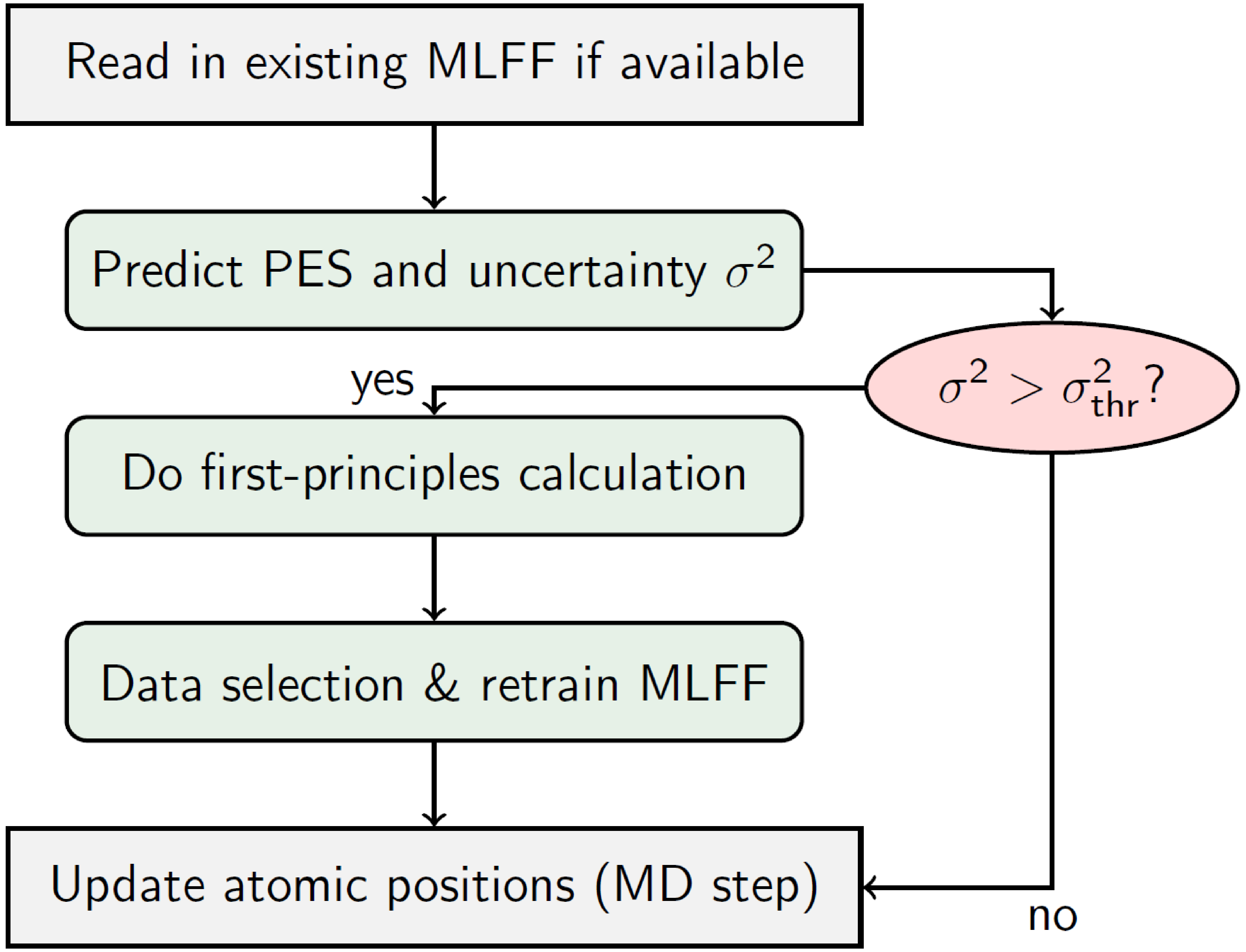

Outlook

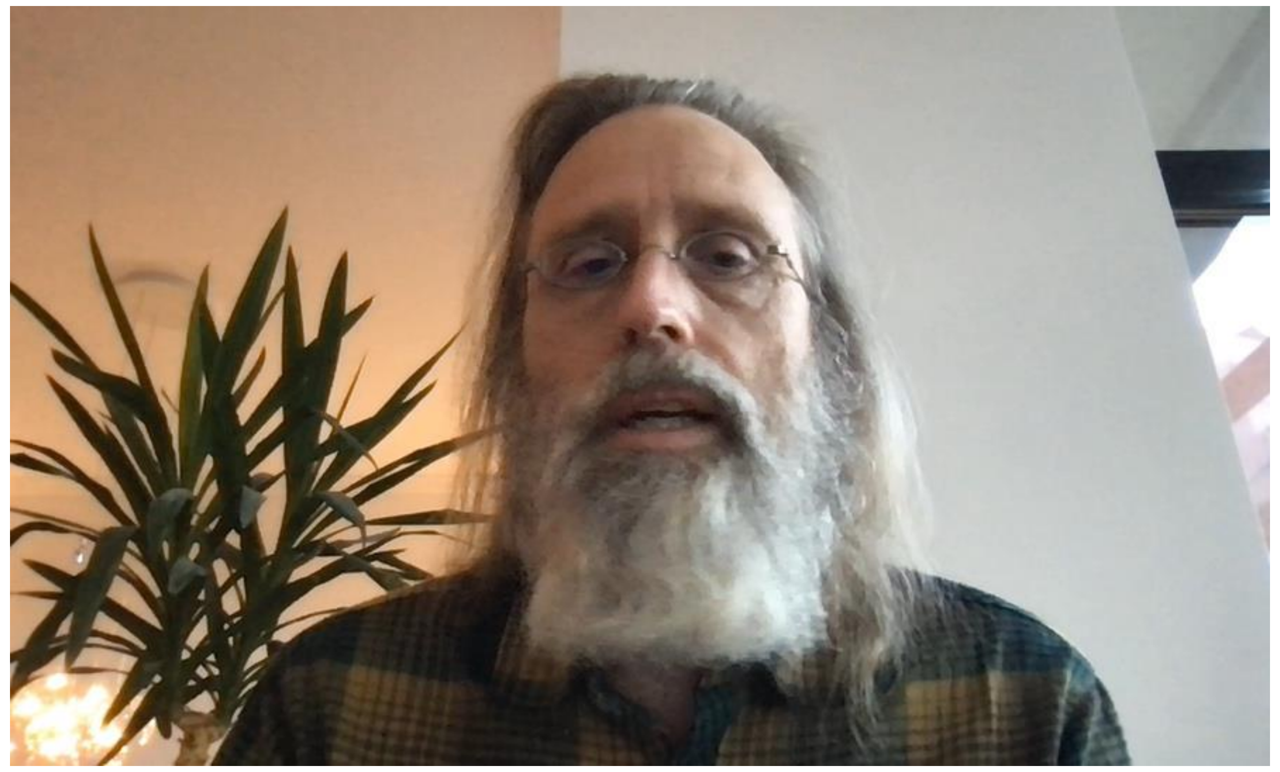

- MLFF interface for LAMMPS
- Other descriptors
- Neural networks
- More observables

- Python plugins

- Support for AMD and Intel GPUs

- And many other things … like for instance electron-phonon coupling!

Question and Answer Session

Dr. Volker Eyert

Materials Design

Professor Georg Kresse, Dr. Martijn Marsman and Dr. Manuel Engel

University of Vienna and VASP GmbH

Announcements

ugm.materialsdesign.com

MedeA Training:

On-the-fly Machine Learned Forcefield with MedeA VASP

Thursday, November 7th

Dr. Shubham Pandey

Materials Design

Question and Answer Session

Dr. Volker Eyert

Materials Design

Professor Georg Kresse, Dr. Martijn Marsman and Dr. Manuel Engel

University of Vienna and VASP GmbH

Questions about Materials Design UGM

Katherine Hollingsworth

khollingsworth@materialsdesign.com

materials design

MedeA

Innovation by Simulation